UNIVERSITY OF CALIFORNIA SAN DIEGO

Adherence-Independent Home Monitoring for the Early Recognition of Impending Hospitalizations:

A dissertation submitted in partial satisfaction of the
requirements for the degree Doctor of Philosophy

in

Bioengineering

by

Nicholas Harrington

Committee in charge:

Kevin King, Chair
Bruce Wheeler, Co-Chair
Parag Agnihotri
Todd Coleman
Sanjoy Dasgupta
Robert Owens

2022

The dissertation of Nicholas Harrington is approved, and it is acceptable in quality and form for publication on microfilm and electronically.

University of California San Diego

2022

TABLE OF CONTENTS

LIST OF FIGURES

LIST OF TABLES

ACKNOWLEDGMENTS

Many people have done so much to prepare me for UCSD and to make my time here enjoyable and challenging. I would like to thank Kevin King, for being such a great mentor these last five years. He was both incredibly knowledgeable and hands on, yet always kind, patient, and understanding. I want to thank my grandparents, Nana and Pops, whose generosity made my college education possible. I also want to thank my family for their love and support. My dad, for his tireless and hard work in running his own business and my mom, for her tireless and hard work to homeschool me and my siblings. I also want to thank my wonderful fiancée Ariel, who will very soon be a part of our family. And finally I want to thank God, "from whom all things came and for whom we live" (Rom. 11:6).

Additionally, I want to recognize several other individuals for their contributions to this research in particular. AJ Wassell was instrumental due to his work installing our devices in patient's homes. Brandon Hernandez-Pacheco and Zhe Wei were diligent and hard working undergraduate students who worked on various aspects of this project. I also want to thank Sean Pawlicki for his assistance in the design and manufacturing of our devices, as well as Mike McCauley for his open source BCM2835 library.

Chapter 3 is largely a reprint of portions of material as it appears in "Passive longitudinal weight and cardiopulmonary monitoring in the home bed". Harrington N, Bui Q, Wei Z, Hernandez-Pacheco B, DeYoung PN, Wassell A, Duwaik B, Desai AS, Bhatt DL, Agnihotri P, Owens RL, Coleman T, King KR. Nature Scientific Reports, December 2021. The dissertation author was the primary investigator and author of this paper.

Chapter 4 is largely a reprint of portions of material as it appears in the following manuscript prepared for submission: “Nocturnal Respiratory Rate in 22,000 Sleep Studies”, Harrington N, Barba DT, Hernandez-Pacheco, B, King KR. The dissertation author is the primary investigator and author of this paper.

Chapter 5 is largely a reprint of portions of material as it appears in the following manuscript prepared for submission: “Nocturnal Respiratory Rate Dynamics as Biomarkers of Impending Hospitalizations”, Harrington N, Barba DT, Bui Q, Wassell A, Khurana S, Rubarth RB, Sung K, Owens RL, Agnihotri P, King KR. The dissertation author was the primary investigator and author of this paper.

Chapter 6 contains portions of material as it appears in the following manuscripts prepared for submission: “Development of sepsis in the home bed”, Harrington N, Agnihotri P, King KR. The dissertation author was the primary investigator and author of this paper. “Development of an acute pulmonary embolism in the home bed”, Barba DT, Harrington N, Agnihotri P, King KR. The dissertation author was the secondary author of this paper.

The Hispanic Community Health Study/Study of Latinos (HCHS/SOL) was performed as a collaborative study supported by contracts from the NHLBI to the University of North Carolina (N01-HC65233), University of Miami (N01-HC65234), Albert Einstein College of Medicine (N01-HC65235), Northwestern University (N01-HC65236), and San Diego State University (N01-HC65237) (AG05407, AR35582, AG05394, AR35584, AR35583, AG08415). The National Sleep Research Resource was supported by the National Heart, Lung, and Blood Institute (R24 HL114473, 75N92019R002).

The National Heart, Lung, and Blood Institute provided funding for the ancillary MrOS Sleep Study, "Outcomes of Sleep Disorders in Older Men," under the following grant numbers: R01 HL071194, R01 HL070848, R01 HL070847, R01 HL070842, R01 HL070841, R01 HL070837, R01 HL070838, and R01 HL070839. The National Sleep Research Resource was supported by the National Heart, Lung, and Blood Institute (R24 HL114473, 75N92019R002).

The Multi-Ethnic Study of Atherosclerosis (MESA) Sleep Ancillary study was funded by NIH-NHLBI Association of Sleep Disorders with Cardiovascular Health Across Ethnic Groups (RO1 HL098433). MESA is supported by NHLBI funded contracts HHSN268201500003I, N01-HC-95159, N01-HC-95160, N01-HC-95161, N01-HC-95162, N01-HC-95163, N01-HC-95164, N01-HC-95165, N01-HC-95166, N01-HC-95167, N01-HC-95168 and N01-HC-95169 from the National Heart, Lung, and Blood Institute, and by cooperative agreements UL1-TR-000040, UL1-TR-001079, and UL1-TR-001420 funded by NCATS. The National Sleep Research Resource was supported by the National Heart, Lung, and Blood Institute (R24 HL114473, 75N92019R002).

The Sleep Heart Health Study (SHHS) was supported by National Heart, Lung, and Blood Institute cooperative agreements U01HL53916 (University of California, Davis), U01HL53931 (New York University), U01HL53934 (University of Minnesota), U01HL53937 and U01HL64360 (Johns Hopkins University), U01HL53938 (University of Arizona), U01HL53940 (University of Washington), U01HL53941 (Boston University), and U01HL63463 (Case Western Reserve University). The National Sleep Research Resource was supported by the National Heart, Lung, and Blood Institute (R24 HL114473, 75N92019R002).

This Wisconsin Sleep Cohort Study was supported by the U.S. National Institutes of Health, National Heart, Lung, and Blood Institute (R01HL62252), National Institute on Aging (R01AG036838, R01AG058680), and the National Center for Research Resources (1UL1RR025011). The National Sleep Research Resource was supported by the U.S. National Institutes of Health, National Heart Lung and Blood Institute (R24 HL114473, 75N92019R002).

VITA

2015-2017	Undergraduate Research Assistant, University of California San Diego
2017	Bachelor of Science, University of California San Diego
2017-2022	Graduate Research Assistant, University of California San Diego
2018-2019	Teaching Assistant, University of California San Diego
2022	Doctor of Philosophy, University of California San Diego

ABSTRACT OF THE DISSERTATION

Adherence-Independent Home Monitoring for the Early Recognition of Impending Hospitalizations

by

Nicholas Harrington

Doctor of Philosophy in Bioengineering

University of California San Diego, 2022

Professor Kevin King, Chair
Professor Bruce Wheeler, Co-Chair

Rehospitalizations for chronic diseases such as heart failure are common and costly. However, they are also preventable. In many cases, timely interventions can prevent the patient from reaching a critical point where hospitalization is needed. Since these decompensations occur necessarily in the patient's home, home health solutions are an ideal choice to give clinicians insight into their patient's well being and enable timely interventions. However, many home health solutions are limited by requiring adherence or technological literacy, or in some cases, an invasive procedure. We describe here a non-contact adherence-independent system for

total body weight and cardiopulmonary monitoring in the home bed (BedScales). We describe the system design and present validation experiments. Additionally, we discovered that nocturnal respiratory rate (NRR) in particular is a very useful, yet understudied biomarker for detecting disease exacerbations. We therefore performed the first large-scale analysis of NRR from over 22,000 sleep studies and found that there is an association between NRR and chronic diseases such as atrial fibrillation, heart failure, and COPD. We installed BedScales devices in the homes of high-risk patients and monitored them for an average of one hundred days each. In doing so, we found instances where NRR rose from baseline in response to diseases such as sepsis, pneumonia, and heart failure. Finally, we present three case reports from patients we monitored with complex physiology, demonstrating how the BedScales platform and NRR would be able to greatly expand the window that clinicians had for performing a timely intervention. We believe that this approach to outpatient management will be able to, in a practical and widely applicable manner, allow clinicians to care for their patients at home and achieve the triple aim of improving care, improving quality of life, and lowering costs.

Chapter 1: Introduction

This dissertation focuses on the development of a sensor and analytics platform designed to give advanced warning of exacerbations of chronic disease, and investigates nocturnal respiratory rate as a powerful but overlooked biomarker of patient decompensation.

In this chapter, I will begin by motivating the research. I will describe how improving outpatient care could increase patient quality of life and lower costs. I will then survey some of the current home health solutions and highlight their key limitations. That will lead to an overview of BedScales, our solution to at-home patient monitoring. I will briefly describe what our platform is and what we have accomplished. I will then describe the initial biomarkers we looked at and how nocturnal respiratory rate emerged as a powerful yet understudied biomarker for guiding disease management for patients at home. Finally, I will close with an outline of the rest of the dissertation.

1.1 Hospitalizations and outpatient care

Many individuals suffering from chronic diseases (e.g., heart failure, arrhythmias, COPD) have complex and turbulent physiology as well as recurrent hospitalizations. Although hospital care is necessary for treatment of many illnesses, it is associated with increased functional disability and decreased quality of life, particularly when hospitalizations are repeated and prolonged. Fortunately, many hospitalizations are avoidable with early recognition and intervention. Heart failure for example, is among the most challenging chronic conditions to manage. It affects more than 6 million patients in the US and costs more than $30B per year, largely due to the high burden of inpatient care required to manage recurrent exacerbations (1).

These hospitalizations are not always without warning and are often preceded by fluid accumulation with congestion and associated shortness of breath. If identified early, heart failure exacerbations can often be managed in the outpatient setting with temporary intensification of diuretic therapy (2) (3).

Outpatient care therefore has an enormous strategic advantage since the physiologic changes that precede these rehospitalizations occur necessarily outside of the clinic, i.e. at home. These changes, however, are opaque to clinicians who can only observe and provide care for their patients in the narrow window, and artificial setting, of a clinic or hospital. Providing doctors a window into this significant aspect of a patient's life would greatly improve their ability to provide care that is timely and proactive. Relying on patients to self-recognize and report symptoms is ineffective, as symptoms are notoriously difficult to self-recognize because they are subjective, gradual, lagging indicators of illness (4). In addition, patients are also often reluctant to disclose symptoms out of fear that they may require hospitalization, a problem that was aggravated by the SARS-CoV-2 pandemic (5). If pre-symptomatic prodromes of hospitalization could be recognized in the home, diagnostic workup and/or treatment could begin earlier, in lower acuity care settings, potentially reducing the number, duration, and complexity of hospitalizations.

The potential for early intervention is particularly attractive for cardiopulmonary diseases such as heart failure, COPD, and pneumonia, which represent the most common causes of hospitalizations in older adults. These patients often present with respiratory symptomatology, are distinguishable based on history (with or without blood tests and a chest x-ray), and are associated with well-established interventions that can be administered in clinic or

at home (6–9). For example, diuretics are often uptitrated for heart failure exacerbations; bronchodilators, steroids, and antimicrobials are administered for COPD exacerbations; and antibiotics are initiated for early uncomplicated bacterial respiratory infections (7, 8, 10). In some cases these decompensations, such as that of a heart failure patient transitioning from euvolumia to hypervolumia (sometimes by as much as 20 pounds of fluid), do not happen overnight, and a proper understanding of the patient's health at home is a critical step in performing the necessary intervention in a timely manner. Outpatient management therefore is a critical area where improvements in patient monitoring could both lower costs and increase quality of care.

1.2 Home health

Attempts have been made to address these issues by home-health solutions. Care coordinators, for example, manage large cohorts of patients and schedule home or clinic visits if a patient reports concerning symptoms. However, this method is hindered because the care coordinator must manually contact each patient, limiting the number of patients a single person can look after. In addition, it requires an actively involved patient or family member, and often relies solely on the patient's ability to correctly identify and communicate symptoms in a timely enough manner for an intervention to be effective.

Various technological solutions could be used to alleviate this problem, but they almost always require the patient to adhere to daily measurements or data transmission, a task that for very sick patients is not possible, and even for healthy individuals is difficult to do consistently across many months. For example, wearables are limited by the need for patient engagement to charge and utilize sensors and apps (11) (12). Implantable devices, such as CardioMEMs have

proven to be useful, but still require patients to adhere to daily transmission of the data (13–15). In managing heart failure for example, a study of telehealth was performed in which each subject was instructed to call in and describe symptoms and provide information like weight. However, even despite an aggressive reminder system, 15% of the subjects never made a single call, and adherence to daily measurements dropped to 55% after 6 months (16). In the status quo, therefore, there are a large number of avoidable rehospitalizations for common yet difficult to manage diseases. Awareness of an impending clinical event is difficult to acquire because it is time-consuming and haphazard to do manually, and is limited by patient adherence to using technology. There is a need then to give clinicians better insight into their patient's condition at home in a manner that is versatile enough to be used in a wide variety of home settings and that overcomes the critical adherence barrier.

1.3 BedScales

We set out to solve this problem by developing a system of sensors and analytics that monitor patient physiology in-home. The goal was not to create an entirely novel type of sensor, but rather was to create a new system of hardware and software that was actually useful outside of the laboratory, and thus was sensitive to all of the real world concerns involved. We required our design to be fully automated and non-contact to overcome the adherence barrier and be applicable to individuals who are very sick. We required the system to be inexpensive and durable, such that it could be deployed in hundreds of real world settings. We required the system to provide easy to understand results, so that clinicians would not be bogged down by a large amount of new, and difficult to interpret, data.

Our sensors are small scales placed under the patient's bed that collect physiologic data continuously while the patient sleeps. We transmit this data to the cloud, process it through a pipeline of analytics, and surface the results to a web-based dashboard for care coordinators to review. This allows care coordinators to target their calls and home visits to the most critically ill patients, greatly expanding the scope of patients they can care for as well as providing the research community with information on the prodromes of disease exacerbations in the home. We developed visualization tools and a risk score in order to surface this information to clinicians in an easy to digest manner. We developed this solution to be applicable to the vast majority of patients, and thus require no patient participation or technological literacy. We used simple components and an injection molded housing which enables us to produce our devices on a large enough scale that they can be used in the real world to impact patient management. We have installed these devices in over 50 homes around the San Diego area and have collected over 5,000 nights of data. Throughout the process, we have worked with care coordinators, in one case alerting them to an impending decompensation that upon a visit to the clinic was discovered to be an undetected pulmonary embolism (see section 6.3).

1.4 Biomarkers of disease

We began development of our solution by focusing on heart failure in particular and to do so, we targeted weight, respiratory signals, and ballistocardiograms (BCG), a mechanical cardiac signal caused by the ballistic motion of the heart (correlated with stroke volume and contractility), as the key biomarkers to acquire. Weight is relevant for heart failure patients because they often suffer from volume overload brought on by a weakened heart squeeze being interpreted by the kidneys as low blood pressure. Respiratory rate is relevant to heart failure

patients as volume overload can cause pulmonary edema and heart failure patents are often short of breath. Heart rate is relevant for heart failure patients due to the presence of tachypnea and arrhythmias. Passive home monitoring of some of these biomarkers has been achieved, but never all three by the same sensor. For example, by embedding sensors into a wide range of everyday objects, measurements have been made of respiratory signals and BCG signals from healthy individuals and patients with chronic diseases (17–21). A modified stand-upon weigh scale was shown to classify heart failure patients based on 30 second BCGs, but the short duration of monitoring and the requirement for patient-initiated self-measurement leave it vulnerable to poor patient adherence (22–24). Smart scales can record and transmit daily weight but still require the patient to diligently use them. Respirations and BCGs are often measured by piezoelectric or electromechanical film sensors placed above or below mattresses or bed frames, or via bedside radio frequency transmit-receivers (25–29); however, because these sensors do not span the entire body and are primarily sensitive to high frequency dynamic signals, they are unable to measure total body weight, which can increase prior to a heart failure hospitalization (30).

1.5 Nocturnal respiratory rate

As we developed our system, we found that nocturnal respiratory rate (NRR) in particular emerged as a powerful biomarker. We found that patients had consistent night-to-night distributions of NRR that were stable across time and varied from patient to patient. This low-noise background is ideal to detect an underlying change in physiology that may herald a disease exacerbation. In our cohort of patients we observed elevated NRR days to weeks prior to hospitalizations for diseases such as sepsis, pneumonia, and heart failure. Additionally, we

found that in general NRR is an under-studied biomarker. Its dynamics are not characterized longitudinally nor are its statistics analyzed across populations. In awake individuals, its interpretation is complicated by its dependence on voluntary effort, activity level, effort, and emotion (31, 32). However, during sleep NRR reflects underlying physiologic and pathophysiologic determinants (33, 34). Furthermore, because NRR strongly impacts inpatient deterioration scores (35–40), it may be useful as a biomarker of impending hospitalization in the home. In order to fill in this gap in the literature, we adapted our analytics pipeline to process data from sleep studies across more than 22,000 subjects. This enabled us to report population level statistic for NRR, and for a subset of over 5,700 patients, to understand the dependencies and relationship of NRR to various clinical variables.

1.6 Scope of dissertation

This dissertation outlines our research starting with the problem of recurrent, avoidable rehospitalizations, all the way to the implementation of a fully automatic, adherence independent system that has been used in patient homes for over two years. We began with the goal of developing a non-contact, adherence independent sensor for weight and using an additional piezoelectric sensor for the high frequency respiratory and cardiac signals. However, when we found that the weight sensor was sensitive even to very small vibrations, we designed our BedScales platform to measure all three signals. Chapter 2 works through key components of this BedScales system, including sensor design, the analytics pipeline, and data visualization. Chapter 3 then reports the validation we did of the three biomarkers against commercial scales and in clinical studies. We found in doing so that all three biomarkers could be monitored by our platform, but that both weight and BCG had significant barriers to being used in real world

settings. However, the respiratory measurement was not only robust in numerous settings, it was information rich and seemed to correspond to patient decompensation. Chapter 4 then narrows in on this biomarker, NRR, in particular and reports its population level statistics, demonstrating its relationship to outcomes, as well as to atrial fibrillation and heart failure. Chapter 5 then focuses in further and characterizes NRR longitudinally in a small cohort of patients and quantifies the visible NRR prodromes of diseases for various hospitalization causes. Chapter 6 focuses in yet again and examines case reports from three individuals with particularly unique and complex medical histories, and demonstrates the benefits that our platform either could, or actually did, bring to their quality of care. Chapter 7 then closes with some remarks on future work and a summary of these results.

Chapter 2: The BedScales Platform

This chapter describes the BedScales sensor and analytics platform (Fig. 2-1). I will start by reviewing the fundamentals of the sensor and data acquisition process and then describe the physical sensor housing. I will then provide an overview of the data analytics pipeline.

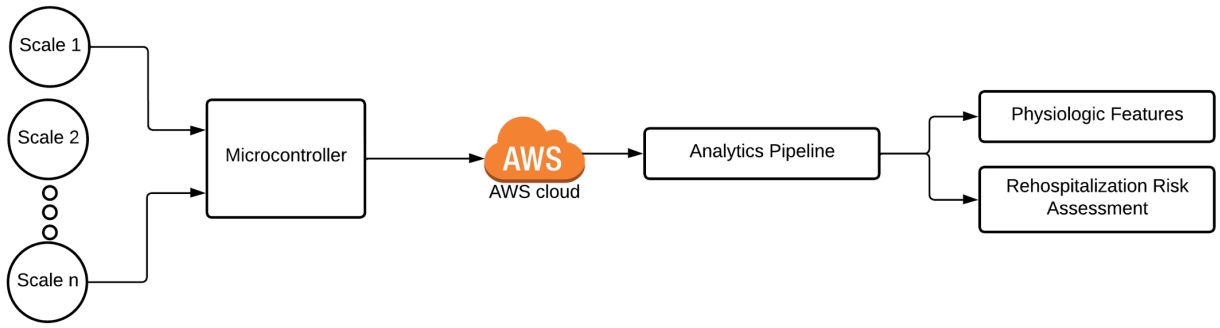

Figure 2-1. BedScales platform diagram. Sensors connect to a microcontroller that reads the data and transmits it to the cloud where it is automatically processed by an analytics pipeline.

2.1 BedScales sensor and data acquisition

In order to measure the weight changes associated with heart failure exacerbations in an adherence independent manner, we needed to leverage something that the patient consistently places their full weight on. We chose the bed as the ideal place to make this measurement. In order to acquire the full body weight, we chose to place the scales under the bed legs, as that would ensure that all of the force from the patient's weight would pass through the legs, through our sensor and into the floor. To be adherence independent, the scales need to monitor constantly since there will be no prior knowledge of when the patient is about to get into bed. We found in preliminary tests that the subtle shifts in a person's center of gravity while they breath, as well as small vibrations from the ballistic motion of a person's heart, are detectable as a oscillating signal on top of the large DC shifts associated with weight. Therefore our weight

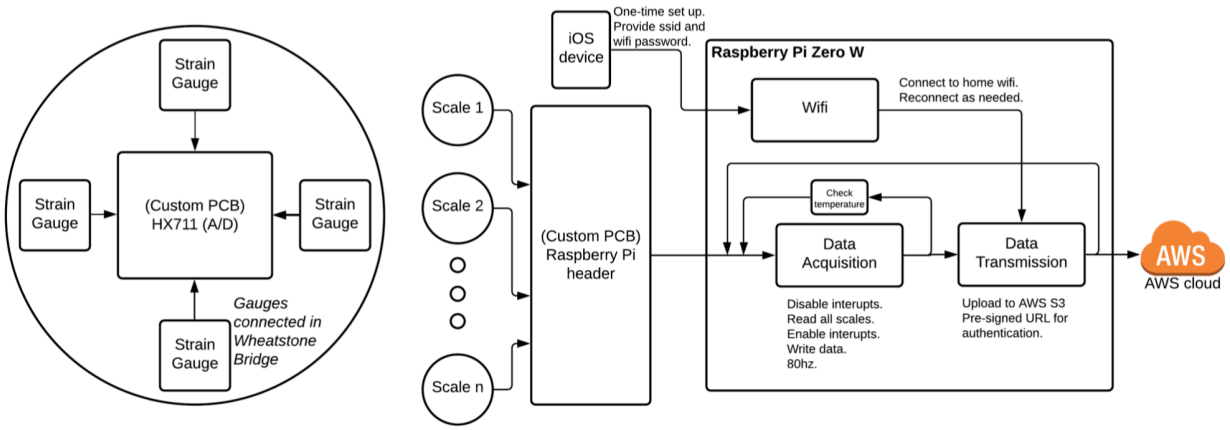

Figure 2-2. Block diagram of BedScales. Scale components (left) and microcontroller (right). The scale is comprised of four strain gauges connected to a PCB. The scales connect to the microcontroller via a custom PCB header. Wifi is set up on the microcontroller via a smartphone app. The microcontroller iterates through data acquisition and hourly data transmission.

sensor will be able to simultaneously measure all three of our target biomarkers. Figure 2-2 shows a diagram of the sensor and microcontroller components. The following subsections outline the circuitry used to make this sensitive measurement of weight, followed by two other subsections that describe the data acquisition process and the physical housing design.

2.1.1 Sensing circuit

Resistors oppose the flow of electrons causing a drop in voltage. The amount of opposition that resistors provide is given by the following equation:

$$R = \frac{\rho L}{A} \tag{1}$$

Where ρ denotes the intrinsic material resistivity, L denotes the length, and A denotes the cross-sectional area. Deformations of a resistor, such as stretching, increase its length and therefore its effective resistance value. Strain gauges are metal components that take advantage of this property by mounting two resistors in series such that as the metal component bends

under an applied load, the flexible resistor deforms with it, thus changing the balance of voltage across the two resistors and converting the applied load into a voltage change.

To create a more sensitive measurement of force, three other resistors can be used along with the strain gauge, in two parallel sets known as a Wheatstone bridge (Fig. 2-3). The relationship between the resistors and applied voltage is given by:

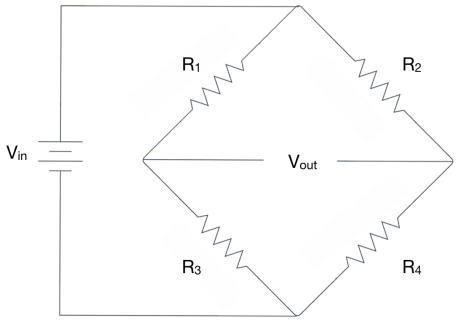

Figure 2-3. Wheatstone bridge circuit diagram.

$$V = (\frac{R1}{R1 + R2} - \frac{R4}{R3 + R4})Vin \quad (2)$$

This balance between the left and the right sides of the bridge is very sensitive to changes in the resistance values, making the Wheatstone bridge an ideal circuit to detect resistance changes due to strain. This property can be further accentuated by using strain gauges for every resistor in the bridge and configuring them such that the voltage on one side of the bridge increases with applied load while the voltage on the other side decreases. This means that even a small load causes a large disparity between the voltages on the right and the left. This precise measurement of force is the backbone of our sensing system. The strain gauges we chose are

strong enough to bear 50kg each, yet within a Wheatstone bridge configuration, they are sensitive enough to detect respiratory and cardiac signals.

2.1.2 Data acquisition

The output of the Wheatstone Bridge is an analog signal and requires an A/D converter to store and transmit the signal. We chose the HX711 (Avia Semiconductor, China) as it is a typical chip for load cell data acquisition. The HX711 provides a variable amount of gain, can sample up to 80Hz, and has a 24 bit A/D converter, allowing for precise measurements. To be used in our system, we needed supporting resistors and capacitors for the HX711, a way to collect and transmit the data from the HX711 to the cloud, as well as the infrastructure to combine four strain gauges into the Wheatstone Bridge configuration. To accomplish this, we created and mass produced a custom PCB (Fig. 2-4a) that supports the HX711, that has solder points for the strain gauges, and a micro USB interface that both provides power and a means to collect the data from the HX711. We did this in CircuitMaker software (Altium, San Diego, CA) using open source HX711 breakout board and load combinator schematics, both from SparkFun (Niwot, CO). We wanted to use a single microcontroller to collect and aggregate data from each sensor and to transmit data over wifi, as enabling each individual sensor to do this would have

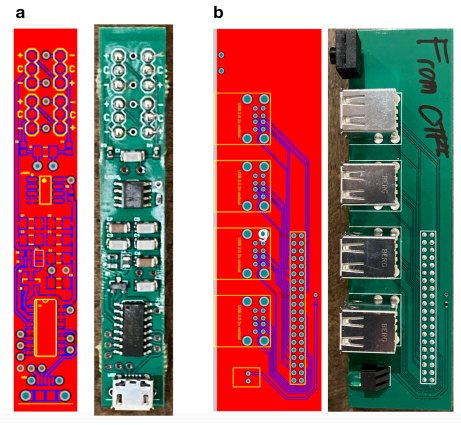

Figure 2-4. Custom PCBs. a, Data acquisition PCB for HX711 and strain gauges. Layout (left) and photo (right). **b,** Microcontroller interface PCB. Layout (left) and photo (right).

unnecessarily increased the cost and complexity of the system. We chose the Raspberry Pi Zero W (Raspberry Pi Foundation, United Kingdom), a small, credit card-sized computer as our microcontroller because of its low cost, ease of use, and small form factor. This microcontroller is both wifi and bluetooth enabled. It was important to make installation as streamlined as possible and since our device has no built-in screen or keypad, that means that the wifi credentials would need to get on the microcontroller via bluetooth. We built a smartphone app to accomplish this, as well as to deposit a token on the microcontroller so that it can connect securely to our Amazon Web Services cloud storage (Seattle, WA). We then needed an interface between the microcontroller and the sensors that was easy-to-use and could account for the fact that different beds have different numbers of legs. To do this, we designed a custom PCB in CircuitMaker that attaches to the microcontroller and supports up to eight USB connections at a time (Fig. 2-4, b).

Once powered on, the microcontroller detects the number of scales connected and reads from each iteratively. We wrote our acquisition script in C++ (using a BCM2835 library from Mike McCauley) so that we could disable and reenable interrupts on the microcontroller while the sensors are being sampled. We chose a transmission frequency of one hour to balance the need to transmit data frequently, so that patient decompensations could be noticed in near real-time, while also not transmitting so often that the data acquisition frequency was so slow as to lose the high frequency cardiac signals.

2.1.3 Injection molded housing

In order to use under a patient's bed, the strain gauges and PCB all need to be secured into a housing that could withstand the weight of the bed and ensure that the force was directed

through the sensors. We modified an earlier metal prototype and designed and mass produced a custom injection molded plastic housing that is strong enough to bear the load of the bed, yet can be produced inexpensively at large quantities and is easy to assemble (Fig. 2-5a) (Solid Works, Dassault Systèmes, France) (Pawli Products, San Diego, CA). We ordered custom dies (Alpha Die Cutting, San Diego, CA) to make rubber pads for the top and bottom of the housing to avoid sliding or damaging the floor (Fig. 2-5, c-d). We also designed and mass produced an injection molded housing for the microcontroller with an indicator light (Fig. 2-5b).

In order to get accurate load measurements from the scale, it is crucial that the force applied to the top of the housing only passes through the strain gauges, into the housing feet,

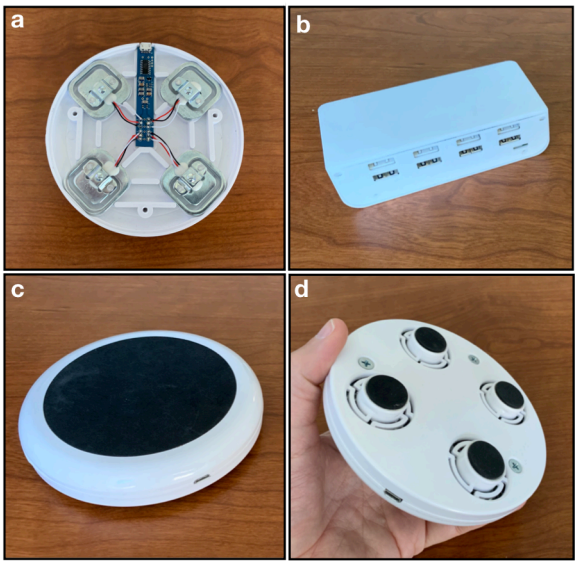

Figure 2-5. BedScales housing design. a, Inside of single scale showing PCB and strain gauges. **b,** Microcontroller housing with ports for scales to connect through. **c,** Top of single scale, showing rubber pad on top. **d,** Bottom of single scale, showing rubber feet.

and ultimately into the floor (and is not shunted to any part of the housing). We observed a spring-like mechanism in commercial bathroom scales and created a similar mechanism for our

device (Fig. 2-6). This holds the feet securely over the center ball of the strain gauge, yet gives them flexibility to rotate and does not restrict movement in the z axis, which is the axis of strain being measured. We also noticed in commercial scales, and used in our own design, a small metal insert as the point of contact between the strain gauge and the feet, to reduce the plastic deformation over time. In this section then, we have gone from the fundamental ideas of resistors causing a voltage drop, to a circuit that is sensitive to applied load, to a method of reading and digitizing this voltage frequently and precisely, to then putting all of that into an easy to manufacture housing. This completes the hardware portion of the platform.

Figure 2-6. Sensor detail. Spring mechanism and metal insert on inside of bottom scale plate.

2.2 Data analytics pipeline

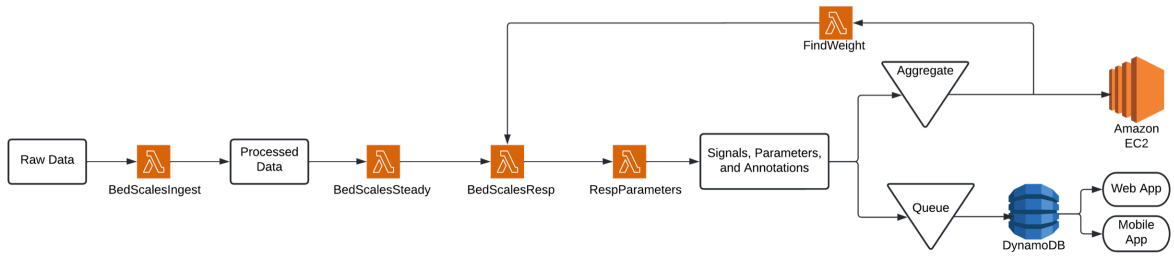

Figure 2-7. BedScales analytics pipeline. Raw data is ingested, steady regions are found, peaks and valleys are annotated, and parameters are found. The resulting data is then aggregated into single-night files to find weight to feed back into the pipeline and the resulting data is downsampled and stored in the backend of our web app and smartphone app.

In this section, I will describe the processing pipeline that transforms raw voltage readings from our sensor into meaningful physiological parameters that can be used to guide clinical care. When designing the pipeline architecture, the key challenges were that in order for this system to be useful outside of the laboratory, the pipeline needed to operate in real time and be scalable. Care coordinators need to know as soon as possible when a patient is in critical condition, and our system needs to perform well when used by thousands of patients. These constraints mean that many things that would normally be acceptable in a research setting, such as asynchronous processing, patient-specific parameter tuning, and manual supervision, were not options for us. We needed a pipeline that would run automatically, regardless of who was using the sensors and regardless of how many devices were installed.

To accomplish our goals, we chose Amazon Web Service's Lambda Functions for our pipeline infrastructure. These functions are containers for our Python scripts that run when triggered. When a function is trigged (by the placement of a file in a specific cloud storage

location for example), a computing instance spins up, runs our script to process the file that triggered it, and then turns off. If hundreds of files are deposited at once, then hundreds of instances will spin up, all running the same script on different files. This allows our pipeline to be massively parallel as thousands of instances can all simultaneously process incoming data. We chained several of these functions together to create our pipelines. Figure 2-7 shows our pipeline for processing respiratory signals from BedScales devices. The first function, BedScalesIngest, takes raw files and pre-processes them. The second, BedScalesSteady, finds stable, low variance regions. The third, BedScalesResp, derives a single respiratory signal with peaks and valleys labeled. The final function, RespParameters, converts this information into meaningful features like respiratory rate, defined at constant intervals (i.e. every 30 seconds). The resulting data is then fed into an aggregate queue, to combine all hours within a night into a single file for future processing/visualization and the resulting data is fed into a database queue, where it is deposited in the backend of our web and mobile apps.

2.2.1 Limited assumption approach

The key challenge in creating this pipeline was how little could be assumed about the incoming data. We did not want to assume a certain number of scales per patient, since beds have a variable numbers of legs, and scales may need to be added or removed, so we made the pre-processing function detect the scale number automatically. We could not assume when the person was in bed, as people have vastly different sleep schedules and patterns. We used a weight threshold to detect if the patient was in bed, but to find this threshold, we could not assume a range of weights that would apply across all individuals and all installations. Even patient-specific weight values would need to be updated periodically if a scale became

disconnected or broken, or if the patient's weight changed by a sufficient amount. We also needed this threshold to be relative to the patient's own "out-of-bed" baseline, since that will depend on the specifics of the installation. To solve these issues, we built an additional portion of the pipeline to aggregate all the files from a given night and use the result to estimate the relative weight of the person in bed and that installation's baseline value. That threshold is then used as a starting point for all of the files in the subsequent night. This allows the pipeline to still work in real time based on an automatically detected patient weight estimate, yet also adapt across time if this threshold needs to be updated. Once we knew when a patient was in bed, we still could not assume that physiology was present as movement artifacts greatly perturb the subtle signals from respiration or BCGs. This is why we have a function to find stable regions placed prior to the peak finding function, to ensure that peaks and valleys are only labeled when the signal is stable enough to be physiology. Finding these peaks and valleys, however, brought up additional issues as the standard, "find_peaks" function from SciPy seemed to use parameters that needed to be slightly tuned to the signal in question. To solve this, we wrote a custom peak finding script (based on the SciPy "find_peaks" function) that was more agnostic to the signal magnitude. Since these are physiologic signals we are processing, however, we do have some prior knowledge about what is a feasible result , so we required the peak finder to give rise to respiratory rates greater than six brpm. To turn those peaks and valleys into a respiratory rate, we needed to be careful to not let errant peaks contaminate our estimates, so we used the median inter-breath interval within a moving window as our primary means of estimating the respiratory rate.

2.3 Data visualization

After processing the data, we then are left with a large number of parameter epochs per night. However, digesting all this data in an understandable matter is difficult. A graph of a single parameter like NRR across one night gives a good sense of the intranight dynamics, but does not represent the bulk of the longitudinal data. Each patient would need to be represented by hundreds of graphs to see the full picture. Whereas a graph of nightly NRR averages gives a good sense of the internight changes but that reduces a very information-rich picture of thousands of NRR epochs per night into a single value. Our solution was to use heatmaps to display NRR (or any other parameter that we calculate). Figure 2-8 shows the progression of

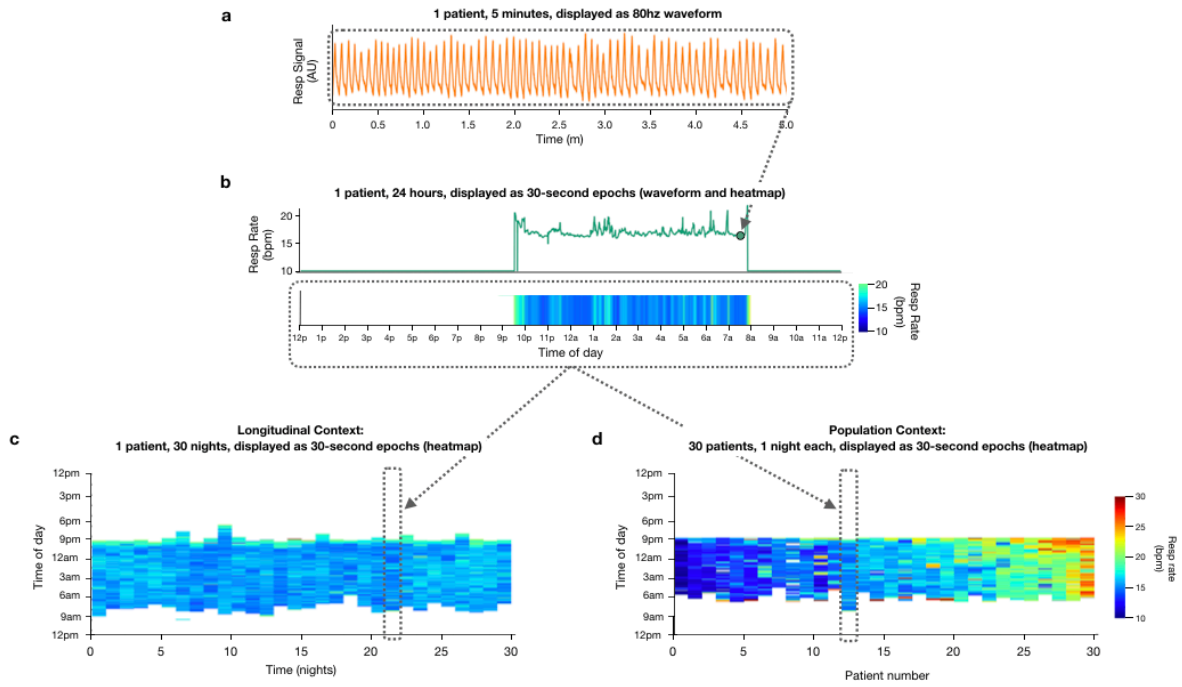

Figure 2-8. Heatmaps as a tool to visualize nocturnal respiratory rate. a, Five minute segment of a respiratory signal. **b,** 24-hours of respiratory rate epochs, depicted as a graph and as a color bar. **c,** Composite heatmap showing NRR longitudinally, 30 nights for 1 patient. **d,** Composite heatmap showing NRR across a population. 30 patients, 1 night each.

how a segment of respiratory signal can be turned into 24 hours of parameters displayed either as a plot or a heatmap where color corresponds to respiratory rate magnitude. Then, by rotating and stacking many such heatmaps horizontally, we create a composite heatmap picture of NRR across time, allowing color to fully show the intranight and internight variations simultaneously. We have found this to be a powerful tool, a colorful “fingerprint” of a patient, as their NRR patterns evolve across time, allowing us to “at-a-glance” take in thousands of hours of data.

2.4 Conclusion

In conclusion, here we describe a non-contact adherence independent sensor system for monitoring weight, respirations, and BCG in the home bed. We overcame challenges in the hardware and software domains to produce an inexpensive, easy to manufacture, fully automated home-health sensor with the goal of providing clinicians with better insight into patient trajectories at home.

Chapter 3: BedScales Validation

In this chapter I present validation experiments for weight, respiratory, and cardiac monitoring using the BedScales platform. The following sections are portions of our paper published in *Scientific Reports*. In that paper we validated our ability to measure weight across multiple weeks and across a wide range of weight values. We validated our respiratory rate measurements by comparing them to a chest belt in clinical sleep studies. We validated our BCG signals by comparing them to electrocardiograms (ECG) in clinical sleep studies. After presenting these proof-of-concept results, I will discuss where each biomarker stands in terms of its ability to be successfully monitored in-home and then provide details of the methods employed.

3.1 Results

In this section I cover the three main biomarkers, weight, respiratory rate, and heart rate that the BedScales platform was designed to monitor. We performed proof-of-concept validation with each of these useful biomarkers.

3.1.1 Passive weight monitoring.

Commercial weigh scales require that patients remember to self-initiate daily standing weight measurements and are limited to engaged patients who can safely and stably stand on a home floor scale. Hospital beds measure patient weights when they are in bed using non-contact sensors, but they do so only at a single time point, leaving them vulnerable to unmeasured errors when blankets, pillows, books, and devices are added between the time of zeroing and

measuring weight. In contrast, the benefit of BedScales is that they are designed to measure the weight of the bed and its contents continuously across time, which will allow for separate quantification of persons and objects based on the times that they are added or removed. For example, one can see the separate addition of a glass, increasing amounts of water, and recurrent placement and removal of a smartphone (Fig. A-1). Weights are measured by summing the loads measured by the sensors beneath each bed leg. When an inanimate object of constant weight is moved to different locations on the bed, to simulate a person changing positions, the distribution of load amongst the sensors changes, but the total measured weight remains relatively constant (Fig. 3-1a). Figure 3-1b illustrates the individual sensor measurements (color) and their sum (black) while a person is awake using a laptop compared to after they fall asleep. Note that movements become infrequent and episodic during sleep. Validation studies demonstrate that BedScales weight estimates are linearly correlated with commercial floor scales across clinically relevant weight ranges (spanning 100–800 lbs) (Fig. 3-1, d-f). These value represent an average of three bedscales measurements per sample and are fit to the commercial scales using two point calibration. Additional characterization studies examining the lower limits of sensitivity demonstrated the ability to discern changes of 0.03 lbs and measure light-weight objects (e.g., smartphone) that are commonly placed onto the bed (Fig. A-1). Figure 3-1g shows a comparison of several weeks of daily weights measured by the BedScales compared to two commercial floor scales (each with a reported accuracy of ~ 0.2 lbs).

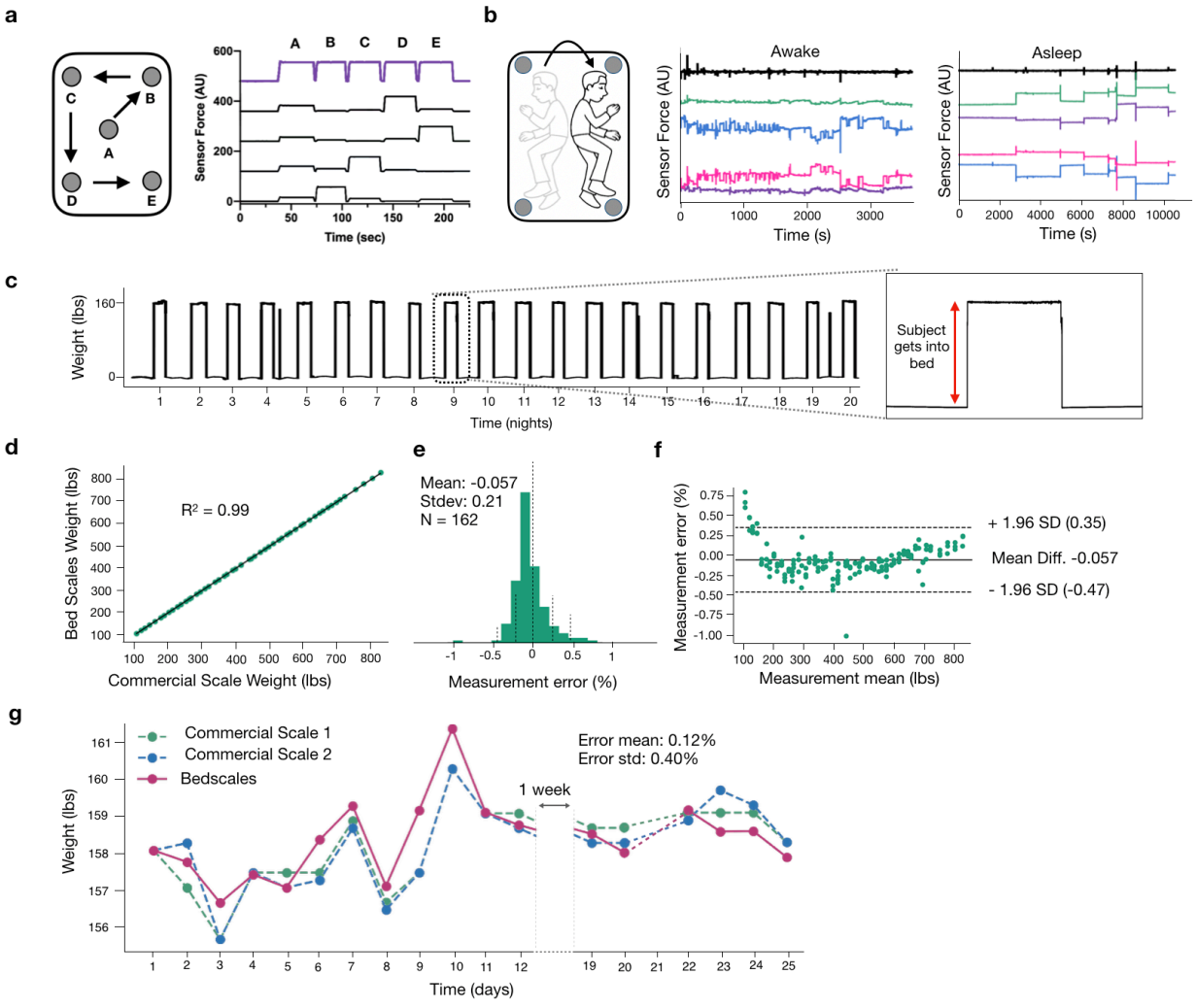

Figure 3-1. Non-contact adherence-independent longitudinal weight monitoring. a, Measurement of individual (black) and summed (purple) sensor loads during movement of a 25 lbs weight from positions A through E (middle to the four corners of the bed). **b,** Cartoon illustrating a sleeping subject redistributing total body weight during episodic movements in bed. Individual (colored) and summed (black) sensor loads are shown while a subject is awake in bed using a laptop with frequent redistributions of load (left) and during sleep with only episodic movements separated by long periods of lying still (right). **c,** 3 weeks of the longitudinal sum of scales used to derive daily weights. Inset shows a single day of a person getting into and out of bed. **d,** Correlation plot of BedScales versus commercial floor scale weights (n = 162). **e-f,** Histogram and Bland–Altman of measurement error, expressed as a percent of measured weight, comparing BedScales versus commercial floor scale. **g,** Comparison of daily BedScales weight measurements compared to two commercial bathroom scales. Pairwise error mean (0.12% or ~ 0.2 lbs) and standard deviation (0.40% or ~ 0.6 lbs) are shown.

3.1.2 Passive weight monitoring of multiple individuals sharing a bed.

Individuals often share the bed with a partner or pet (Fig. 3-2a); and we reasoned those weights could be separately inferred based on the timing differences between their getting into and out of bed (Fig. 3-2b). To determine the minimum interval that would allow discrimination of two-person weights, we performed simultaneity tests in which two persons entered and exited the bed at successively decreasing time intervals (Fig. 3-2c). Even when the interval was reduced from 30 seconds to 5 seconds, the two individuals were readily discriminated and weighed (Fig. 3-2, d-g). While further work would need to be done to write an algorithm that can separate the weights automatically, this demonstrates that from a sensor perspective, BedScales could be used to measure total body weight in a patient's home bed, even if the bed is shared with a partner or a pet.

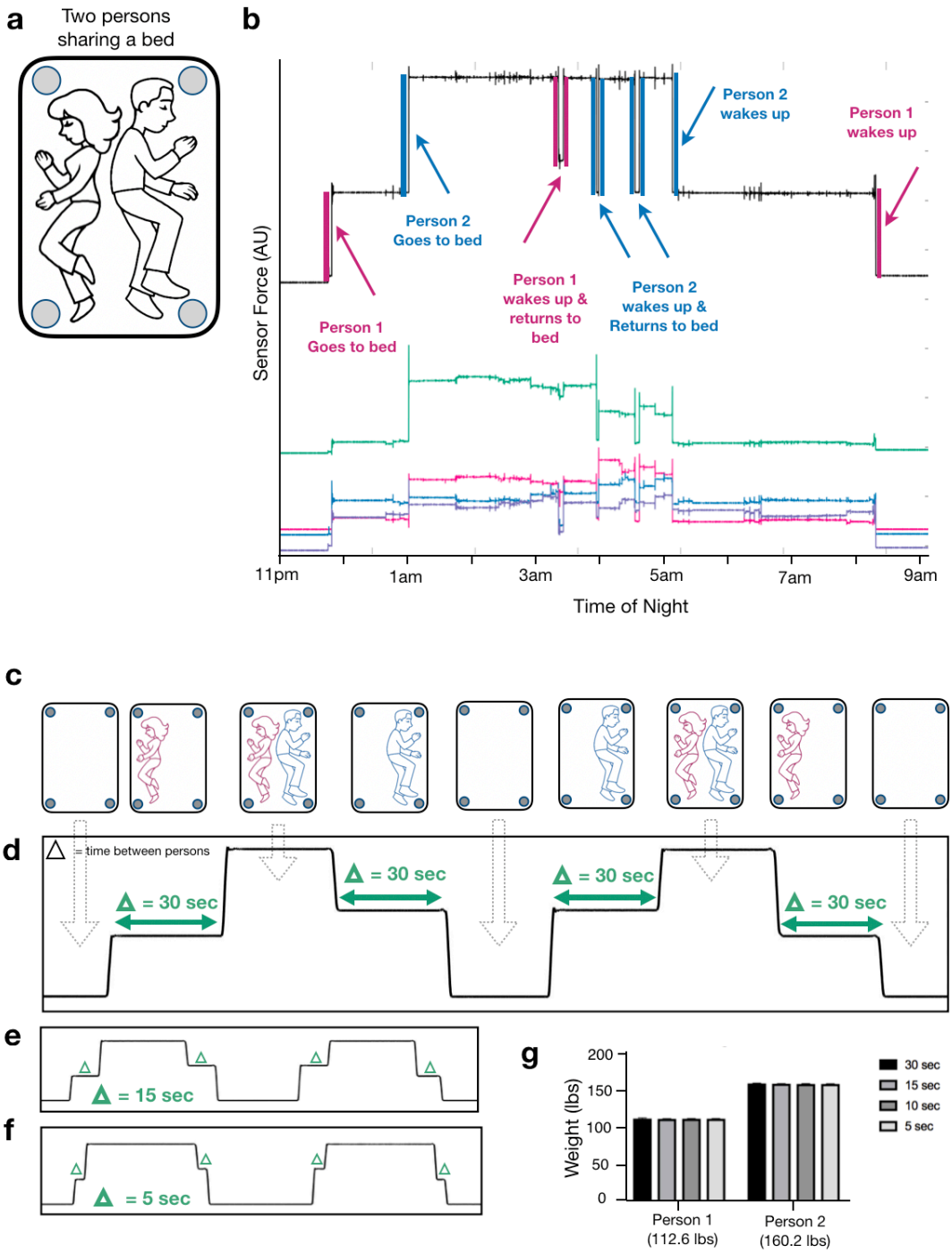

Figure 3-2. Non-contact adherence-independent multi-person weight monitoring. a, Cartoon of partners sharing a bed. **b,** Overnight measurements of two partners sharing a bed. Colored signals indicate individual sensor tracings. Black indicates the sum of sensors. Sudden weight changes due to each person getting into and out of the bed are color coded (blue and pink) and annotated. **c,** Illustration of synchronicity protocol for measuring total body weights at progressively shorter time intervals. (Person = P) P1 On, P2 On, P1 Off, P2 Off, then repeated exchanging P1 and P2. **d,** Corresponding total weight signal measured by the BedScales with a time interval of 30 s, **e,** 15 s, and **f,** 5 s. **g,** Estimates of decoupled weights of the two individuals sharing a bed for each synchronicity time interval and corresponding weight measured by a commercial floor scale (mean + standard deviation).

3.1.3 Respiratory monitoring using non−contact bed sensors.

When a patient is asleep in bed, episodic musculoskeletal movements are separated by comparatively long movement-free intervals during which low variance physiological signals such as respirations and ballistocardiograms can be measured. This provides opportunities to perform quantification of respiratory rate and detection of episodic tachypneas, apneas, and periodic breathing. BedScales respiratory signals arise from the dynamic redistributions of load that accompany chest wall movement during inspiration and expiration. To convert signals from multiple sensors into a single patient respiratory signal, we first performed bandpass frequency-dependent filtering of the individual sensor signals (cutoffs at 0.167 Hz and 1.5 Hz). We then had separate signals from each sensor that needed to be combined into a single composite respiratory signal. To do this, we used principal component analysis within a sliding window to calculate eigenvalues that, when multiplied by individual sensor signals and algebraically summed, create a maximally variant single respiratory source signal for peak finding (Fig. 3-3, a-b). The resulting signal enabled quantification of interbreath intervals and respiratory rates.

Respiratory signals exhibited expected contours with brisk linear upstrokes during inspiration followed by exponential decays during expiration (Fig. 3-3, b). To validate the measurements, we installed BedScales beneath the legs of a hospital bed during overnight sleep studies and compared the resulting signal to those obtained from the standard commercial chest belt respirometer (Fig. 3-3, b-c). To facilitate comparisons, we estimated the respiratory rate every 30 seconds generating 5737 respiratory rate epochs from 8 patients and observed a mean error and standard deviation of -0.17 ± 0.72 bpm. This is shown longitudinally across time (for a single patient) (Fig. 3-3c) as a histogram of errors (Fig. 3-3d), and as a Bland–Altman plot

(Fig. 3-3e). Additionally, we have placed in Appendix A, two more analyses that we performed on the respiratory signal. We explored a method for demixing the respiratory signals from two individuals sharing a bed (Fig. A-2) and we also found that BedScales can monitor more complex respiratory patters and, for a single patient, quantified the burden of sleep apneas through the lens of BedScales (Fig. A-3).

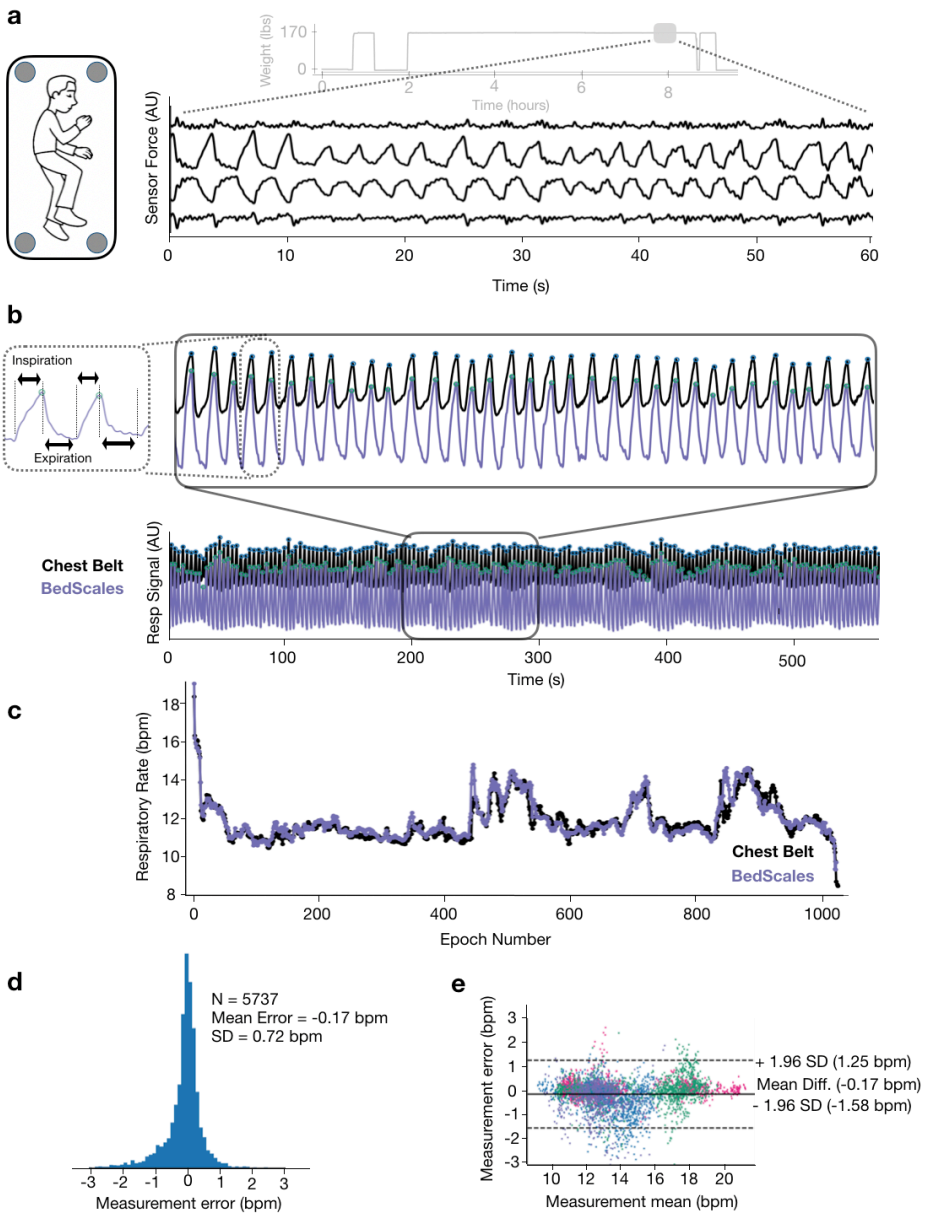

Figure 3-3. Respiratory monitoring using non-contact adherence-independent BedScales. a, Raw respiratory signals from 4 scales in the middle of an overnight recording (light gray is the entire overnight weight signal). **b,** Composite signal (purple) derived from linear combination of scales weighted by PCA-based eigenvalues compared to commercial respiratory chest belt (black) with peak finding annotation (green and blue dots respectively) across short (top) and long (bottom) time scales. Inset shows short inspiratory phase with rapid linear increase during inspiration followed by longer exponential decay during passive expiration. **c,** Comparison of respiratory rates derived from BedScales (purple) and commercial respiratory chest belt (black) across one night (~ 1000 epochs). **d,** Histogram of respiratory rate differences between BedScales and a commercial respiratory chest belt across 8 sleep study patients. X axis limits set at ± 1% quantile of error. **e,** Bland–Altman plot comparing BedScales and chest belt respiratory rates. Y axis limits set at ± 1% quantile of error.

3.1.4 Heart rate monitoring using non−contact bed sensors.

The mechanical force of each heartbeat results in a characteristic signal known as the BCG with defined waves that follow each QRS complex of the ECG (41). Bandpass filtering of BedScales signals (5 Hz and 50 Hz cutoffs) revealed characteristic BCG morphologies from the individual scales (Fig. 3-4, a-b). A single-peak BCG was derived by converting the raw BCG signal from each scale into an absolute measure of BCG energy (via a smoothed moving variance algorithm). The signals were then summed and filtered (bandpass, 1 Hz, 50 Hz) to create a final single-peak BCG signal, which was used for peak finding, heart rate estimation, and comparison to ground truth ECG-derived heart rates (Fig. 3-4, c-d). We validated the BedScales heart rate estimations by comparing to simultaneously recorded ECGs. Heart rate estimates were made every 30 seconds, which generated 5219 epochs from eight patients. The data showed quantitative agreement with a mean error and standard deviation of -0.94 ± 2.14 bpm, which is displayed longitudinally across time (for a single patient) (Fig. 3-4d), as a histogram of errors (Fig. 3-4e), and as a Bland–Altman plot (Fig. 3-4f). Furthermore, we have placed in Appendix A preliminary results that suggests that complex cardiac features, such as increased stroke volume following a premature ventricular contraction (PVC) or non-sustained ventricular tachycardia (NSVT) are also visible through the lens of Bedscales (Fig. A-4)

.

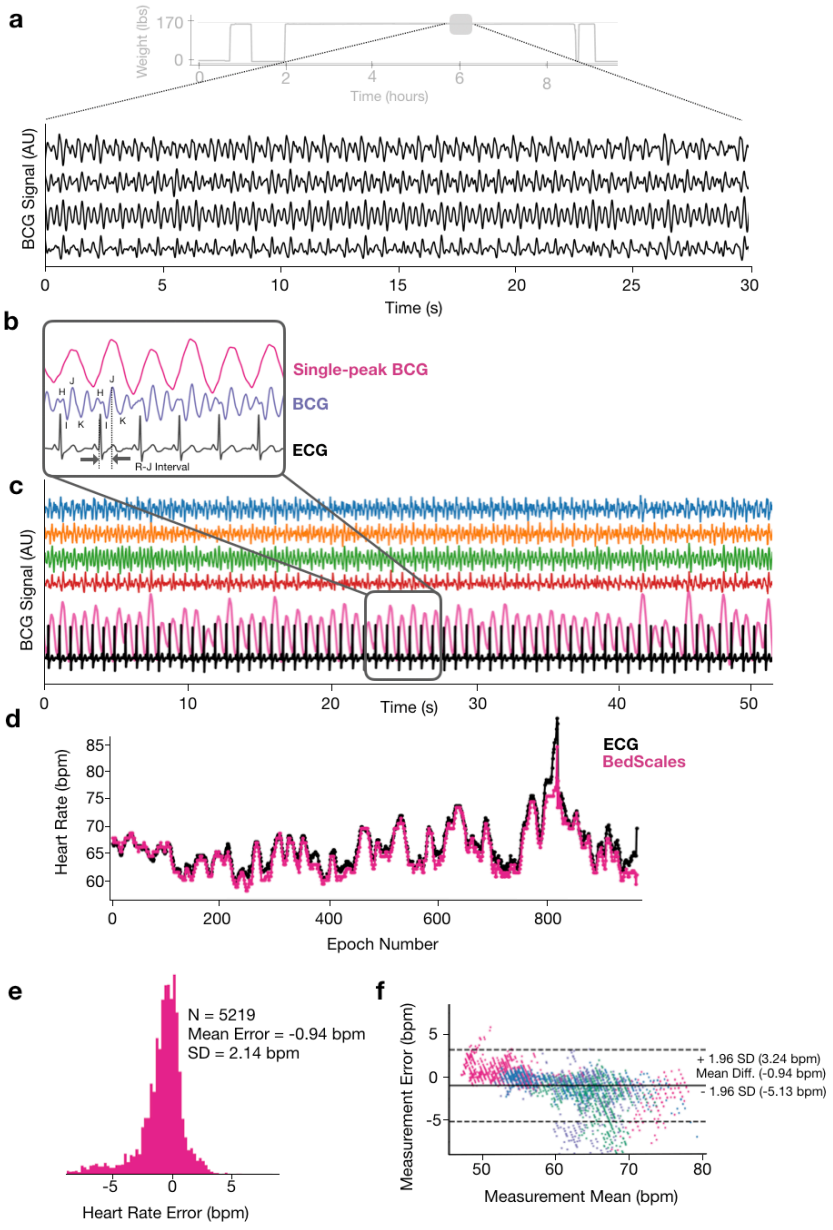

Figure 3-4. Adherence-independent longitudinal ballistocardiographic monitoring using BedScales. a, BCG signals (black) from each of the 4 legs during an overnight recording, smoothed for display (light gray is the overnight weight signal). **b,** Single-peak BCG (pink), BCG (purple) showing the labeled waveform (smoothed for display), and simultaneously recorded ECG signal (black). **c,** Comparison of longitudinal BCG signals from the 4 individual scales (blue, orange, green, red), the single-peak BCG (pink), and the ECG (black). **d,** Comparison of heart rates derived from BedScales (pink) and ECG (black) across one night (~ 900 epochs). **e,** Histogram of heart rate differences derived from BedScales and from ECG across 8 sleep study patients (5219 epochs, mean error −0.94 bpm, standard deviation 2.14 bpm). X axis limits set at ± 1% quantile of error. **f,** Bland–Altman plot comparing BedScales and ECG derived heart rates. Y axis limits set at ± 1% quantile of error.

3.2 Discussion

Here, we describe validation experiments for BedScales, a non-contact adherence-independent sensor designed to longitudinally quantify cardiopulmonary dynamics and weight throughout each night. We found that while both weight and BCG still have significant barriers to being operationalized, the respiratory measured has proven to be incredibly robust in many different situations.

For weight, we have shown that BedScales correlates over large ranges (100-800 lbs), which will be necessary for measuring a large diversity of patients and beds. Additionally, across a longer term, multi-week experiment, the platform in a non-contact manner performed comparably to commercial scales. However, we have in other experiments found that the weight measurement could have some position dependency or even drift over time (the weight measurement changing due to plastic deformation), thus making accurate estimates difficult. Additionally, we have written an algorithm to separate out objects and individuals but that will need to be refined and validated to operationalize this system for patients who share a bed.

For BCG, we have shown that BedScales can match ECG recordings in clinical sleep studies. This is an important result as ECG sensors require the attachments of several electrodes to the patients, whereas BedScales can likewise track heart rate by simply placing our sensors under the bed. However, we have observed that the quality of the BCG signal can depend on the type of bed used, and varies from person to person, such that many of our in-home patients did not have a discernible BCG signal.

We have shown preliminary results in Appendix A of demixing the respiratory signal from two individuals but more work is needed to implement and validate that method in real-time, and it would need to be done for the BCG signal as well.

The respiratory signal however, has consistently performed well in numerous settings. In beds, in recliners, and across multiple years of monitoring, the respiratory signal has been information rich and robust, even when some of the scales become disconnected or break.

Taken together, these results indicate that while the weight and BCG components of the system need further work, or need to be done using an alternate sensor like a piezo electric mattress sensor, the BedScales platform can reliably measure an information rich biomarker across time in an adherence independent manner. The following chapter will take a step back and examine this biomarker in the population, and then Chapter 5 will present our findings from deploying BedScales sensors to numerous patients and observing longitudinally changes in NRR in condition with clinical events.

3.3 Methods

In this section, I will go more in depth as to how the analyses in the above sections were performed.

3.3.1 Human subjects.

The governing IRB for this research was IRB # 171480 and IRB # 180160.

3.3.2 Weight measurement.

Bed sensor weight validation was performed by using five healthy volunteers and two static weights in various permutations to span a large range of loads. Each person was measured

on a commercial bathroom scale before sitting/lying on a bed with the BedScales sensor under each of its 4 legs. The 4 scales were calibrated together by fitting coefficients that minimized the variance when the same load was applied in different places. The final weights were calculated by subtracting the total load measured after and before each permutation of individuals and weights was placed on the bed (3 measurements were made of each permutation and these were averaged together). Two-point calibration that minimized the measurement error was then used to convert from arbitrary units (AU) to pounds (lbs). Longitudinal weight comparisons were made by installing BedScales under a home bed and comparing to self-measurement on two separate commercial floor scales at the beginning of each night of sleep. The limits of sensitivity were tested by placing the sensors beneath a 4-leg couch and placing an empty glass on a flat cutting board. At 20 s intervals, 15 mL (0.033lbs) aliquots of water were added. The glass was removed and replaced with and without water, and a smartphone was repeatedly added and removed.

3.3.3 Two−person weight demixing.

The weights of persons sharing a bed were determined by measuring the calibrated sum of all sensors across time and extracting the large differential weight changes. The weight changes were then classified into two groups termed person 1 and person 2. Simultaneity tests were performed by instructing 2 persons to get into and out of bed at specified temporal intervals in the following sequence—Person 1 (IN), Person 2 (IN), Person 1 (OUT), Person 2 (OUT) and then repeated but exchanging Person 1 and 2. To explore the limits of simultaneity that would still permit decoupling of person weights, we systematically decreased the interval between Person 1 then 2 (or 2 then 1) getting into and out of bed and repeated the experiment

for several time intervals (30 s, 15 s, 10 s, and 5 s), until the maneuver could not reach a steady position in the allotted interval.

3.3.4 Respiratory measurement.

BedScales respiratory signals were generated by frequency-dependent filtering with cutoffs of 0.167 Hz and 1.5 Hz. A single respiratory signal was derived by linearly combining the individual sensor respiratory signals weighted by PCA eigenvalues calculated for each 12.5 s window. A moving variance algorithm was used to isolate regions of steady physiology (regions < 10 s were rejected) and peak finding was performed on these regions. The respiratory rate was calculated using the median inter-peak interval during a 5-min moving window with a shift of 30 s. For validation, the BedScales respiratory signal and chest belt were subject to additional smoothing (moving mean, 0.5 s), windows were required to have no more than 45 s of unstable physiology, and regions with technical artifacts in the chest belt were excluded. Data was aligned and compared to a simultaneously recorded respiratory chest belt with respiratory rates quantified using the same method described above.

3.3.5 Ballistocardiographic measurement.

BCG signals from each scale were derived by frequency-dependent filtering (Butterworth) with cutoffs of 5 Hz and 50 Hz (lower cutoff set to 1 Hz during BCG amplitude analysis). These signals were then smoothed using a moving mean filter and moving variance filters. The resultant signals from each scale were then summed to create a composite signal, which was filtered using another frequency-dependent filter (Butterworth) with cutoffs of 1 Hz and 50 Hz. The resultant signal was a single peak measure of BCG. For in-home data, steady regions (as defined by the respiratory signal) were isolated and analyzed. For validation, a

moving variance algorithm was used to isolate regions of steady physiology (regions < 5 s were rejected) and peak finding was performed on these regions. The heart rate was calculated using the median inter-peak interval during a 5-min moving window with a shift of 30 s. For validation, windows were required to have no more than 45 s of unstable physiology and a region with technical artifacts in the ECG was excluded. Data was aligned and compared to a simultaneously recorded ECG signal with heart rates quantified using the same method described above.

3.3.6 Clinical sleep studies.

BedScales were installed beneath the legs of a conventional hospital bed in the Clinical and Translational Research Institute where overnight sleep studies were conducted. As part of another ongoing study, subjects underwent standard in-laboratory polysomnography (PSG) with electroencephalogram (EEG), electrooculogram, submental and leg electromyogram for sleep staging; nasal pressure and thermistor for airflow measurement; thoracic and abdominal piezoelectric bands for respiratory effort; arterial oxygen saturation monitoring at the finger; and electrocardiogram monitoring for safety. Patients slept supine. Signals from the sleep studies and the BedScales were aligned using custom python scripts.

3.3.7 Statistics.

Statistical analysis was performed using custom python scripts or GraphPad Prism software. All data are represented as mean values±standard deviation unless indicated otherwise. For two-group comparisons, a two-tailed nonparametric Mann–Whitney test was used unless otherwise specified. All analyses except respirophasic inspiratory versus expiratory

BCG magnitudes were unpaired. P values less than 0.05 were considered significant and are indicated by asterisks as follows: *$P < 0.05$, **$P < 0.01$, ***$P < 0.001$, ****$P < 0.0001$.

3.4 Acknowledgements

Chapter 3 is largely a reprint of portions of material as it appears in "Passive longitudinal weight and cardiopulmonary monitoring in the home bed". Harrington N, Bui Q, Wei Z, Hernandez-Pacheco B, DeYoung PN, Wassell A, Duwaik B, Desai AS, Bhatt DL, Agnihotri P, Owens RL, Coleman T, King KR. Nature Scientific Reports, December 2021. The dissertation author was the primary investigator and author of this paper.

Chapter 4: Nocturnal Respiratory Rate and its Relationship to Clinical Variables

In this Chapter, we shift our focus and narrow in on NRR in particular. The previous Chapter described our sensing platform and validation experiments. After deploying our platform in a variety of patient homes, NRR emerged as a potentially powerful biomarker yet not much is known about it. NRR dynamics are not routinely measured at high density in clinical practice. Consequently, the distribution of NRR dynamics in the population or in individuals remains largely uncharacterized. To define NRR in populations, we collected and analyzed raw waveforms from chest belt respirometers or flow sensors from over 22,000 polysomnograms (PSG) from sleep studies taken from the National Sleep Research Resource (42). Here, we present the first large scale analysis of NRR and for a subset of 5700 patients, report its relationship to demographic and clinical data. To do this, we adapted our analytics pipeline described in Chapter 2 to ingest data from the sleep studies, perform peak finding, and find parameters. Due to its parallel and expandable nature, our BedScales pipeline, designed for real-time processing of thousands of patients, is also an ideal tool for retroactively processing large amounts of sleep studies in a reasonable time frame.

4.1 Results

4.1.1 Sleep study analysis

We pulled our PSG data from five sources available on the National Sleep Research Resource. The studies we used were the the Hispanic Community Health Study/Study of

Latinos (HCHS) (43), MrOS Sleep Study (MROS) (44), Multi-Ethnic Study of Atherosclerosis (MESA) (45), Sleep Heart Health Study (SHHS) (46), and the Wisconsin Sleep Cohort Study (WSC) (47).

Figure 4-1, a-b details our basic workflow. We downloaded raw EDF files from each study and processed them through our analytics pipeline to convert the waveforms into signals with annotated peaks and valleys, and then into a series of parameter epochs, defined in 30-seconds intervals. In order to do this, we needed to adapt our pipeline to process data from clinical sleep studies rather than from the BedScales platform. This brought a new set of challenges as we had to make even less assumptions than before. We could no longer isolate steady regions from movements, because the distinction between the two was less clear or predictable as seen from the lens of sleep study data. Additionally, we no longer had access to the weight signal so we needed a new method to tell when the patient was in bed.

We solved both of these problems by creating a new Lambda function that outputs parameters to discern physiology. In particular, we found that by comparing couplets of normalized "breaths" within a moving window, true breaths (those that arise from a stable respiratory signal) were well correlated with each other while false breaths (those that arise from a random noise or movement artifact) had no consistent shape and thus were not as well correlated (see section 4.3 below for details). Figure 4-1c shows the distribution of this metric across all epochs from all studies. We found that this distribution was loosely bimodal, with the smaller peak being related to noise and the larger one being related to stable physiology.

In order to used this metric as a filter for noise versus physiology, we set a cut point as the minimum between these two peaks. Figure 4-1d shows examples of tracings from the left and

right of the cut point. Our goal in doing this was not to perfectly separate quality and noisy tracings, but to cut out the bulk of the tracings that were noise, such that when we found aggregate respiratory epoch statistics, they would be uncontaminated. Additionally, by finding statistics based on all of the quality epochs in a given night, we mitigated the risk of our final answer being impacted by errant regions of noise that made it past our quality metric.

However, in addition to only retaining quality epochs, we also wanted the subject-nights that comprised our final distribution to be high quality and reflective of a relatively normal night of sleep, not be representative of only a few minutes of data with the rest being technical artifacts or movement. Therefore, we found the distribution of time each subject had quality data, as seen in Figure 4-1e and removed all nights where the subject was below the 0.05 percentile for time spent in bed, rounded to the nearest hour (3 hrs). Figure 4-1f shows the amount of nights per study that were initially present (gray) and that were retained (blue).

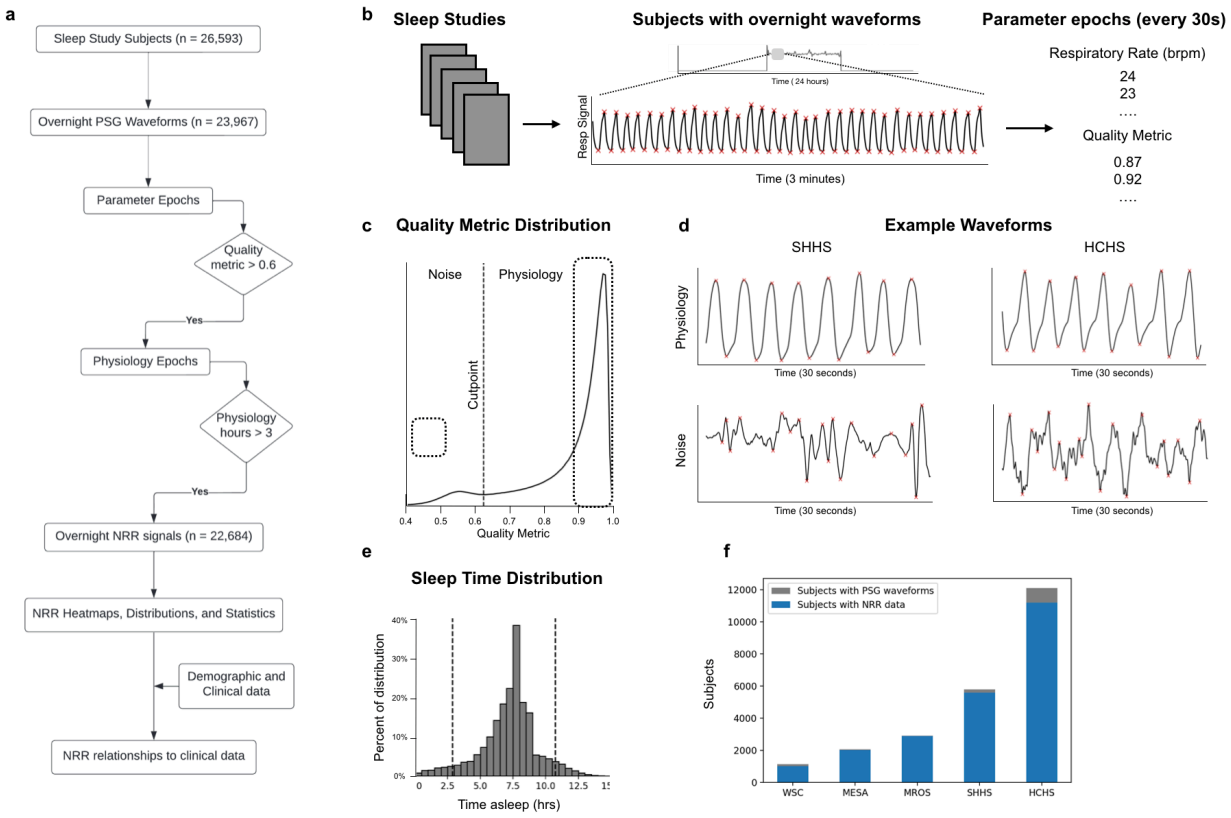

Figure 4-1. Setup and methods for sleep study analysis. a, Block diagram of design of sleep study analysis. **b,** Diagram of studies being transformed into annotated signals, and then transformed into parameters. **c,** Distribution of quality metric across all epochs and all studies. Chosen cut point labeled. **d,** Examples of tracings from the noise side and physiology side of the cut point. **e,** Histogram of time-in-bed of each night in the sleep studies. **f,** Bar plot showing how many nights per study were retained.

4.1.2 Nocturnal respiratory rate in the population

After filtering, we had a resulting 22,684 nights of waveform data to process. Figure 4-2 shows the distributions of these epochs, both as heatmaps and histograms, for each study and then a composite distribution including all of the studies. As described in Figure 2-8d each column of the heatmap represents a single night of data (in this case, a single subject), the y-axis represents the hours in bed (artificially registered so that most studies have the same start time), and the color represents the magnitude of the NRR for that epoch (from 10-30 brpm). We sorted the heatmaps from least to greatest NRR to allow for easier visualization.

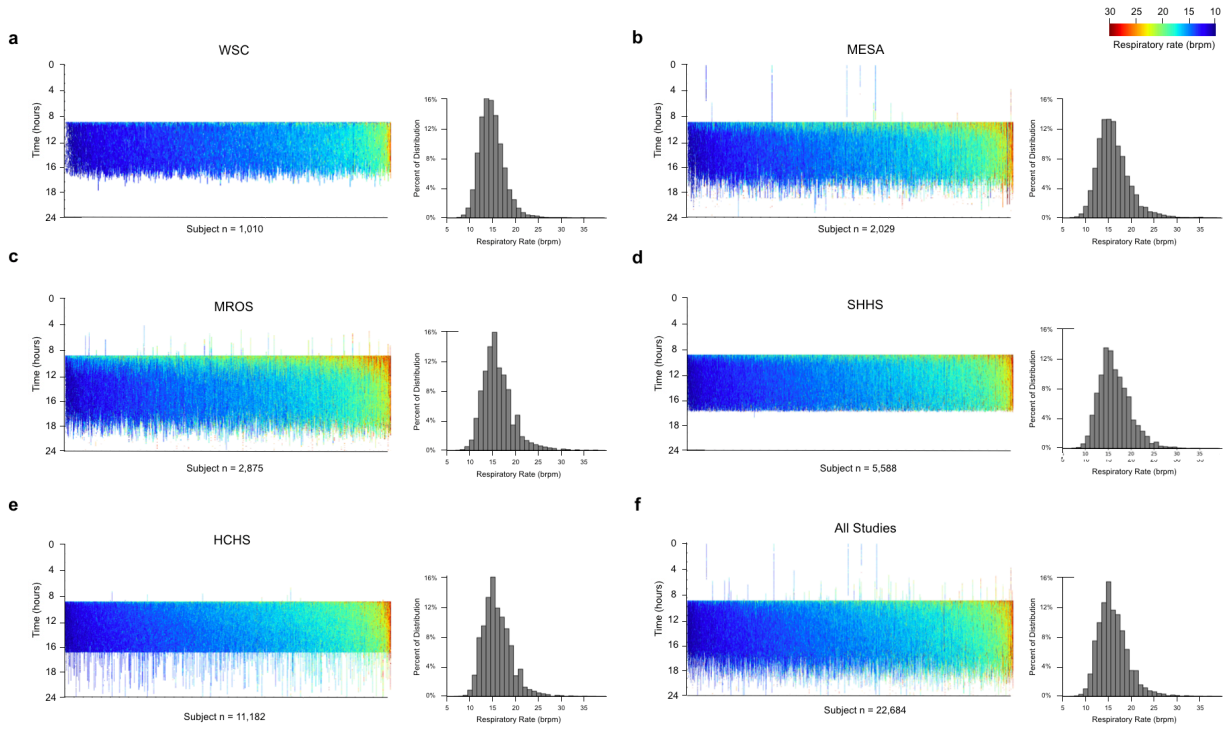

Figure 4-2. NRR distributions displayed as heatmaps and histograms for five sleep studies. Color bar ranges from 10-30 brpm, values below 10 not shown. **a,** Wisconsin Sleep Cohort Study. **b,** Multi-Ethnic Study of Atherosclerosis. **c,** MrOS Sleep Study. **d,** Sleep Heart Health Study. **e,** Hispanic Community Health Study/Study of Latinos. **f,** All sleep studies combined into single distribution.

4.1.3 N Nocturnal respiratory rate relationship to clinical variables

After acquiring the NRR distributions for each study, we created composite statistics (such as mean, median and variance) of the epochs in each night. To understand the relationship that NRR has with other variables, and gain insight into its utility as a biomarker for disease, we then examined the relationship between NRR and key variables in the SHHS study. What follows are preliminary results that we plan to expand to all studies in a future publication. Table 4-1 displays the results. We found that some features, such as age or a history of CABG do not appear to be related to NRR. However, we found that a history of heart failure and atrial fibrillation in particular, as well as COPD, were related to NRR. For example using a cut point of 17 brpm, 4% of all subjects above the threshold had atrial fibrillation, while for those below the threshold, this value dropped to 1%. This may be because NRR is a proxy for interstitial pressure, which is why heart failure and atrial fibrillation had the strongest relationship to an elevated NRR. Regardless, the important take away is that NRR, a biomarker that can be measured in an adherence independent fashion, appears to be linked to chronic diseases of interest. Additionally, NRR also appears to be related to outcomes. Figure 4-3 displays a Kaplan-Meier curve for the SHHS study describing the 15-year survival rates. We separated the patients into 4 different groups based on NRR with cutoffs at 17, 20, and 23 brpm and found that with increasing NRR, groups had less chance of survival, with end-of-study survival rates around 70%, 60%, 40%, and 20% respectively. Figure B-1 in Appendix B presents an odds ratio that communicates a similar relationship between NRR and 15-year mortality.

Table 4-1. Relationship between NRR and demographic/clinic variables.

	High [>17 bpm]	Low [<=17]	P-value
	(N=1568)	(N=4031)	
Age			
Mean (SD)	64.8 (11.9)	62.6 (10.9)	< 1e-04
Median [Min, Max]	66.0 [40.0, 90.0]	62.0 [39.0, 90.0]	
Gender			
Male	772 (49.2%)	1899 (47.1%)	0.1617
Female	796 (50.8%)	2132 (52.9%)	
SBP			
Mean (SD)	129 (19.8)	127 (19.1)	< 1e-04
Median [Min, Max]	127 [79.0, 202]	124 [52.0, 214]	
DBP			
Mean (SD)	73.5 (12.4)	73.7 (11.3)	0.5801
Median [Min, Max]	73.0 [10.0, 120]	73.0 [21.0, 132]	
Height			
Mean (SD)	167 (9.60)	168 (9.57)	0.004969
Median [Min, Max]	167 [145, 188]	167 [145, 188]	
Weight			
Mean (SD)	79.6 (17.1)	77.5 (15.7)	< 1e-04
Median [Min, Max]	78.6 [47.0, 126]	76.4 [47.0, 126]	
BMI			
Mean (SD)	28.9 (5.64)	27.8 (4.81)	< 1e-04
Median [Min, Max]	28.2 [18.0, 50.0]	27.3 [18.0, 50.0]	
Mean Nocturnal Respiratory Rate			
Mean (SD)	19.2 (1.86)	14.9 (1.61)	< 1e-04
Median [Min, Max]	18.7 [16.4, 32.8]	15.0 [9.05, 23.0]	
Median Nocturnal Respiratory Rate			
Mean (SD)	18.9 (1.91)	14.4 (1.56)	< 1e-04
Median [Min, Max]	18.2 [17.0, 33.3]	14.6 [8.51, 16.9]	
Nocturnal Respiratory Rate Variance			
Mean (SD)	4.91 (5.06)	4.43 (5.66)	0.002052
Median [Min, Max]	3.29 [0.367, 52.2]	2.85 [0.219, 107]	
Hx of CABG			
Yes	61 (4.50%)	145 (4.13%)	0.6157
No	1294 (95.5%)	3368 (95.9%)	
RBBB on EKG at visit 1			
Yes	27 (2.45%)	82 (2.84%)	0.5694
No	1075 (97.6%)	2804 (97.2%)	
History of atrial fibrillation			
Yes	39 (4.53%)	25 (1.24%)	< 1e-04
No	822 (95.5%)	1993 (98.8%)	
LBBB on EKG at visit 1			
Yes	18 (1.63%)	26 (0.901%)	0.07018
No	1084 (98.4%)	2860 (99.1%)	
History of heart failure			
Yes	55 (3.68%)	41 (1.07%)	< 1e-04
No	1439 (96.3%)	3803 (98.9%)	
COPD			
Yes	30 (1.97%)	30 (0.755%)	0.0001943
No	1496 (98.0%)	3944 (99.2%)	
Hx of smoking			
Yes	893 (57.5%)	2056 (51.3%)	< 1e-04
No	661 (42.5%)	1953 (48.7%)	

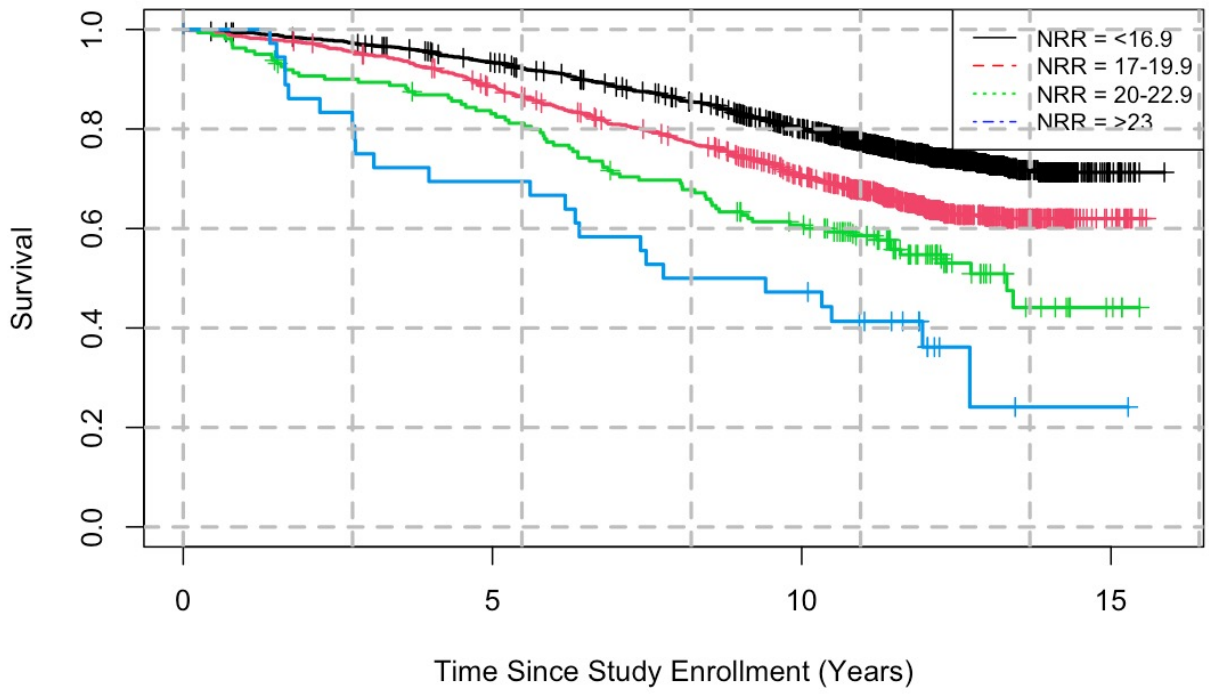

Figure 4-3. Kaplan-Meier curves for NRR. Time is shown on the x axis and survival on the y axis. Colors correspond to individuals with different NRR. After around 2 years, the group with the highest NRR had the lowest percentage of survival at all time points.

4.2 Discussion and conclusion

We present here the first large scale study of NRR. By processing over 22,000 subject nights, we created a novel data set of NRR and its relationship to clinical variables. Our preliminary results have linked NRR in a single study to chronic diseases such as atrial fibrillation as well as to 15-year mortality outcome. Future work will explore the relationships between NRR and clinical variables across all studies. This result is important in the context of our BedScales platform because in the following Chapter, as we return to in-home monitoring, we now have a justification to think that patients with higher NRR are at higher risk, and potentially, that as an individual moves from low to high NRR across time, their physiology may be changing for the worse.

4.3 Methods

4.3.1 Nocturnal respiratory rate estimate and quality metric calculation

The chest belt or flow sensor signals from each study were smoothed (window sizes of 0.5-1 seconds) and peaks were found using a custom peak finding script based on SciPy find_peaks as described in Section 2.2.1. NRR was estimated from the median inter-peak interval within a 5 minute moving window (30 second shift). To derive the NRR quality metric we took all couplets of "breaths" (valley-peak-valley-peak-valley) within a 60 second window (10 second shift) and measured how well each couplet correlated to the others. To do this we normalized the magnitudes, pinned the peaks of each couplet together, resampled the region between them, and truncated the regions on the end such that we would have two couplets, with

aligned peaks, and the exact same number of samples, essentially normalized with respect to time. We then compared each couplet pair with every other couplet pair in the window (using both a Spearman and Pearson correlation calculated using the SciPy package). We then took the median of each type of correlation measure within the window, essentially giving an indication of how well correlated overall the couplets are with each other. To balance the contributions made by each correlation measure, we then took the mean of the two to provide a final single number indicating how overall correlated the couplets are within that 1-minute window. Regions with legitimate physiology should have in general self-similar breaths whereas regions of noise should be far less correlated. To align the NRR and quality metric parameters in time, we then used a 5 minute moving window (30 second shift) to aggregate the quality metric parameters into a single value, defined every 30 seconds, so that there would be a 1-1 match between NRR and our quality metric, enabling easily filtering out of regions that were low quality.

4.3.2 Nocturnal respiratory rate relationship to clinical variables

To create Table 4-1, a Student's t-test and Chi square test methods were used to assess for statistically significant ($p < 0.05$) correlations between "High" (>17 brpm) NRR group and various continuous and categorical clinical variables respectively. For Figure 4-3, Survival analysis performed using Cox regression analysis reveals a decreasing survival rate across increasing NRR groups; highest survival rate in those with NRR < 16.9 brpm and lowest in those with NRR > 23 brpm.

4.4 Acknowledgements

Chapter 4 is largely a reprint of portions of material as it appears in the following manuscript prepared for submission: “Nocturnal Respiratory Rate in 22,000 Sleep Studies”, Harrington N, Barba DT, Hernandez-Pacheco, B, King KR. The dissertation author is the primary investigator and author of this paper.

Chapter 5: Nocturnal Respiratory Rate Enables Early Recognition of Hospitalizations

In this Chapter, we explore NRR dynamics measured by BedScales and evaluate their utility as a biomarker of impending hospitalizations. We deployed BedScales sensors to patient homes and defined high resolution longitudinal NRR trends over months (without requiring any patient participation). This Chapter is largely a reprint of material that we prepared for a manuscript to be submitted in spring of 2022. Our main focus in this Chapter is to examine whether excursions of NRR from patient-specific baselines could be used to recognize some impending hospitalizations before patients report symptoms and whether it could be done without excessive false alarms. In a high-risk, elderly, and medically complex cohort we collected and analyzed 3,403 patient-nights of data (4,326,167 epochs at 30-second intervals) from 34 patients. We found that at nominal alarm thresholds, we detected 11 of 23 hospitalizations, with warning windows ranging up to weeks in advance. Given that only a subset of hospitalizations are expected to have detectable prodromes, this represents a significant improvement over the current standard of patient-reported symptoms. Together, this suggests that NRR may be a useful biomarker for automated early detection of many impending hospitalizations. The following sections report these findings and then conclude with a detailed description of the methods employed.

5.1 Results

5.1.1 Adherence-independent monitoring of nocturnal respiratory rates

To determine the longitudinal patterns of NRR, we analyzed data from an IRB-approved observational study of adherence-independent home bed monitoring. We selected patients enrolled from 6/22/2020 to 1/20/2021 from an academic health center, cardiology practice, and population health program who were felt by their providers to be at high risk of hospitalization for cardiopulmonary causes in the next year (Table 5-1). Patients were on average 75 years old and had multiple co-morbidities. A total of 34 patients were monitored for 3,403 total patient-nights. After removing nights (10%) due to absent or inadequate data, 3,056 patient-days remained for analysis. Participants spanned diverse ages (20's-90's), genders, ethnicities, socioeconomic contexts, body weights, and medical comorbidities; settings ranged from transitional housing, studio apartments, and condos, to multi-story homes in gated subdivisions; and sleep furniture included couches, recliners, and a diversity of beds (twins, queens, kings, and adjacent twins). Problematically, nine of our patients shared a bed with a partner which is discussed more at length in the methods in Section 5.4.2. Many patients suffered from physical or cognitive disabilities that would have made usage of adherence-dependent wearables and mobile apps challenging. For example, we monitored patients with dementia, a woman with blindness from diabetic retinopathy, and another who was bed-bound and neurologically impaired after a debilitating stroke.

Table 5-1. Summary of longitudinal home monitoring patient cohort.

	Full Cohort (34	Admission (16 patients)	No Admission (18 patients)
Age (years)	75.6	74.1	76.9
Gender (Male)	23 (67.6%)	13 (81.3%)	10 (55.6%)
Race (White)	22 (64.7%)	9 (56.3%)	13 (72.2%)
CHF	27 (79.4%)	16 (100%)	11 (61.1%)
LVEF (%)	53.1	47.8	57.8
Body Mass Index (kg/m2)	27.7	28.4	27.1
Atrial Fib/flutter	22 (64.7%)	12 (75%)	10 (55.6%)
Diabetes	15 (44.1%)	7 (43.8%)	8 (44.4%)
Hypertension	29 (85.3%)	15 (93.8%)	14 (77.8%)
Hyperlipidemia	26 (76.5%)	13 (81.3%)	13 (72.2%)
CAD / MI	19 (55.9%)	9 (56.3%)	10 (55.6%)
COPD	12 (35.3%)	6 (37.5%)	6 (33.3%)
Stroke/TIA	8 (23.5%)	5 (31.3%)	3 (16.7%)
Immunosuppressant	6 (17.6%)	4 (25.0%)	2 (11.1%)
Transplant	3 (8.8%)	2 (12.5%)	1 (5.6%)

5.1.2 Longitudinal NRR in patients with clinical stability

In order to understand NRR longitudinally, we divided patients into 2 groups, those who were hospitalized during the period of monitoring and those who were not. We focused first on the patients who were not hospitalized during the analysis period. Individual patients were qualitatively similar to themselves across time but different from other patients as illustrated by four examples (Fig. 5-1, a-d). To analyze the characteristics of stable patients, and to do so in a manner that equally weighted each patient regardless of monitoring duration, we chose 30 nights from each stable patient generating a distribution of around 600,000 epochs, with a mean of 17 brpm and a variance of 16 $brpm^2$ (Fig. 5-1e). Quantitatively, when the distribution of NRRs for individuals were corrected using a universal reference, the variance was significantly greater (15.9 $brpm^2$) than when corrected using a patient-specific reference (7.2 $brpm^2$) (Fig. 5-1f). This suggested that the longitudinal variation for individual patients is low in clinically stable patients. It also suggested that from a practical perspective, detection of excursions from baseline should compare to patient-specific NRR norms rather than cross-sectional population norms, since the interpatient variation was larger than intrapatient variation (Fig. 5-1g).

5.1.3 Longitudinal NRR in patients with hospitalizations and clinical events

We next focused on patients who had clinical events during the monitoring period. During the 3,403 patient-nights of monitoring we observed 23 clinical events, defined as an overnight hospital stay, which is equivalent to a 30-day clinical event rate of ~20%, consistent with the high-risk patient population that we enrolled. We observed hospitalizations for heart failure exacerbation (Fig. 5-2a), pneumonia responsive to antibiotics in a patient with heart failure on dialysis (Fig. 5-2b), failure to thrive in a diabetic man with chronic debilitating

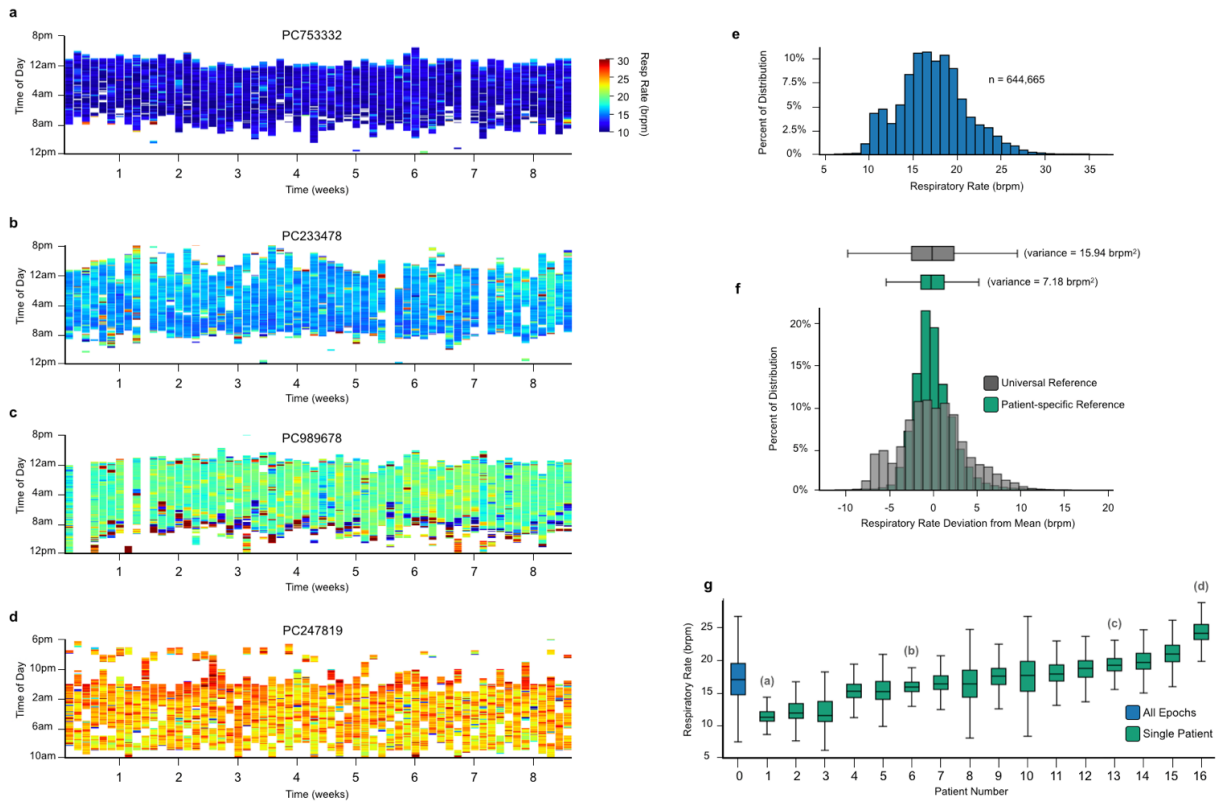

Figure 5-1. Nocturnal Respiratory Rate (NRR) dynamics longitudinally measured in the home bed. a-d, 60-night heatmaps of 4 example patients showing low intrapatient NRR variability but large interpatient NRR differences. Colorbar ranges from 10-30 brpm. Values below 10 brpm not shown. **e,** Histogram of all epochs (n = 644,665) from the 16 clinically stable patients (mean = 17.28 brpm, variance = 15.94 brpm^2). **f,** Histograms of all epochs centered at the universal mean (gray) and each subject centered on their own overall mean (variance = 7.18 brpm^2) (green). For both (e) and (f) the x-ax is cropped such that all bins with >0.01% of data are shown. **g,** Box plot of the entire population as a single distribution (blue) and each individual patient (green). Labels in parenthesis highlight the patients shown in **a-d** with corresponding letter. For the box plots in **f** and **g**, the center line represents the median value, the boxes extend from the first to the third quartile, and the whiskers extend 1.5x the interquartile range before the first quartile and past the third quartile.

musculoskeletal pain (Fig. 5-2c), septic shock in a patient with long standing heart failure on dialysis (Fig. 5-2d), severe anemia from gastrointestinal bleeding in a patient with prior stroke (Fig. C-6, d), as well as community-acquired COVID-19 infection in an immunosuppressed individual, hypoglycemia, hyperglycemia, localized cellulitis, and palpitations due to bigeminy. These clinical events occurred for diverse reasons, only some of which would be expected to have associated changes in respiratory rate.

To analyze the quantitative differences between hospitalized and non-hospitalized patients, we first defined a causal patient-specific baseline as the lowest sustained NRR (see methods in section 5.4.6). We then plotted the deviation of NRR compared to baseline for each patient type. The hospitalized group had a 4-fold greater variance compared to the stable group (3.78 $brpm^2$ and 0.84 $brpm^2$ respectively). The KS statistic for the two groups had a p value <0.0001 indicating that the two distributions were significantly different. By inspection of the cumulative distribution function (CDF), the distinction between the two groups was due to the hospitalized group having a greater proportion of elevations from baseline (Fig. 5-2e). We next asked whether the differences were concentrated in time and localized to the days immediately preceding the hospitalization event. We defined a proximity factor to specify windows in advance of hospitalization for analysis. As the proximity factor decreased, the deviation from baseline increased suggesting that it may be possible to detect impending hospitalization by longitudinally monitoring deviations of NRR from baseline (Fig. 5-2f). We defined a threshold NRR (NRR_{th}) above the patient-specific baseline. When patients exceeded the threshold, they were classified as "in-alarm" (red) while those who remained below threshold were classified as "not in-alarm" (green) (Fig. 5-2g). The optimal value of NRR_{th} can then be selected to maximize detection of impending hospitalizations (true positives) while minimizing alarms for patients who did not ultimately require hospitalization (Fig. 5-2g). We did not classify the latter as "false alarms" since some patients exhibited gradual rise-and-fall patterns of NRR that suggested the presence of a true subclinical event that simply did not require hospitalization but still represented an event that may have benefited from outreach (Fig. C-5). It is important to note that unlike molecular diagnostic tests, which have well-defined ground truths that enable

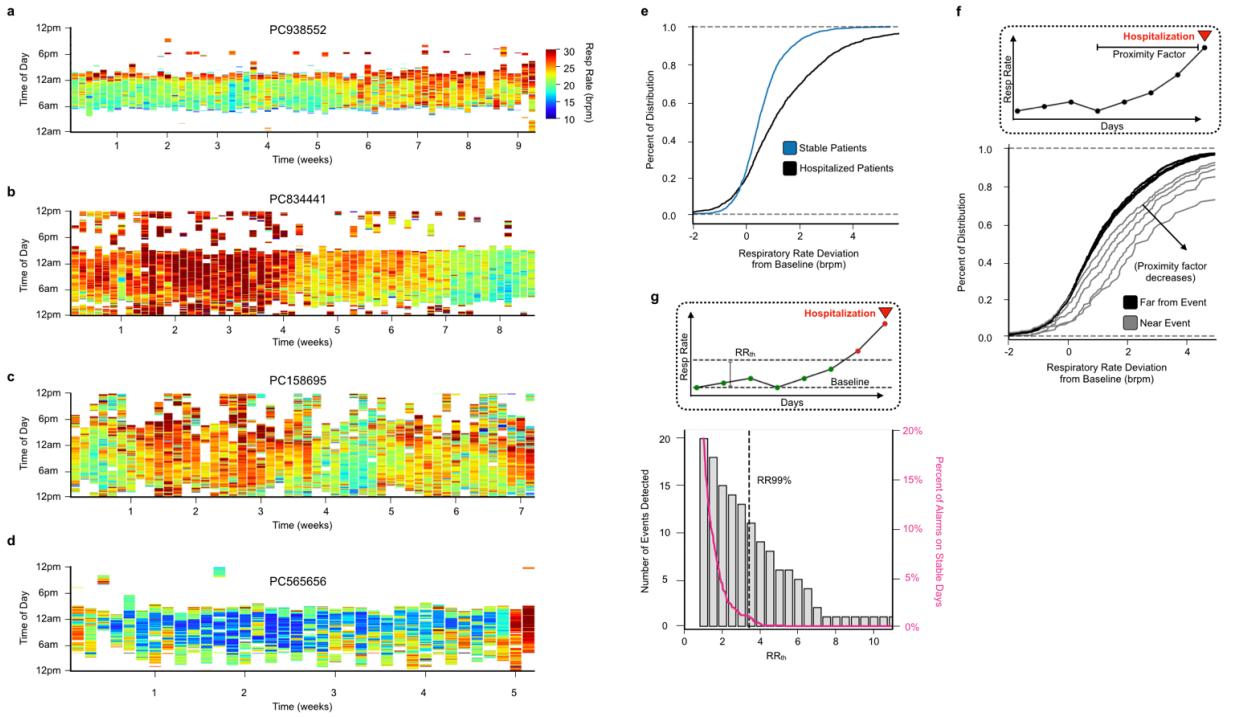

Figure 5-2. Comparison of clinically stable and unstable (hospitalized) patients. a-d, Heatmaps of hospitalized patients. Y-axis is time of day in hours. X-axis is time in weeks. Colorbar ranges from 10-30 brpm. Values below 10 brpm not shown. **e,** CDF of the distribution of baseline deviations for stable patients (blue) and hospitalized patients (black). **f,** Inset shows that the Proximity Factor is a measure of how far a night is from a hospitalization event. Main plot shows a CDF of the distribution of baseline deviations for nights far from a hospitalization event (black), and for nights within 2, 5, 10, 20, and 30 nights from hospitalization event (gray). **g,** Inset shows that the RR_{th} is a threshold with respect to baseline and that days below threshold are considered low risk (green) and days above are high risk (red). Main plot shows the number of hospitalization events detected (gray bars, left y-axis) and the number of days among stable patients that were labeled "high risk" (pink line, right y-axis) for varying values of RR_{th}. $RR_{99\%}$ (black dashed line) is a value of RR_{th} where 99% of stable days are considered low risk.

use of sensitivity and specificity performance metrics, the "impending hospitalization" outcome has no established ground truth. Many hospitalizations would not be expected to have a cardiopulmonary prodrome while many subclinical events that do not reach the level of hospitalization are still worthy of alarm. Therefore, we judged success of NRR based on the ability to maximize the number of detected events per days of monitoring while minimizing alarms for which no subclinical event could be identified.

5.1.4 Development of an impending hospitalization

To evaluate the performance of this approach, we selected a NRR_{th} threshold value to limit above-threshold days to <1% in non-hospitalized patients ($NRR_{99\%}$) and applied it to hospitalized and non-hospitalized patients (Fig. 5-3). This resulted in 2 alarm regions in 2 non-hospitalized patients over 1707 days of monitoring, one of which exhibited a characteristic rise-and-fall pattern suggestive of a true subclinical event for which an alarm would arguably be desired (Fig. C-5), as well as scattered alarms on hospitalized patients but not at a time near their event. By comparison, using a window of 3 days (meaning that events were considered to have been detected if they occurred within 3 days of an alarm) we detected on 11 of 23 hospitalizations, which occurred for reasons including heart failure with volume overload, anemia requiring transfusion, pneumonia, acute COVID-19 infection, and septic shock. To evaluate the window of early detection, we aligned the hospitalization dates and compared the duration of each prodrome. The longest prodrome (~3 weeks) was associated with a volume overload event from heart failure exacerbation. Such warning periods would provide ample time for patient calls, home visits, urgent clinic visits, and escalation of diuretics. Even events with shorter prodromes, if they are disease-like infections, could still enable earlier initiation of antibiotics. This has potential for significant clinical benefit since, every hour of delay in initiating antibiotics is associated with increased mortality in sepsis.

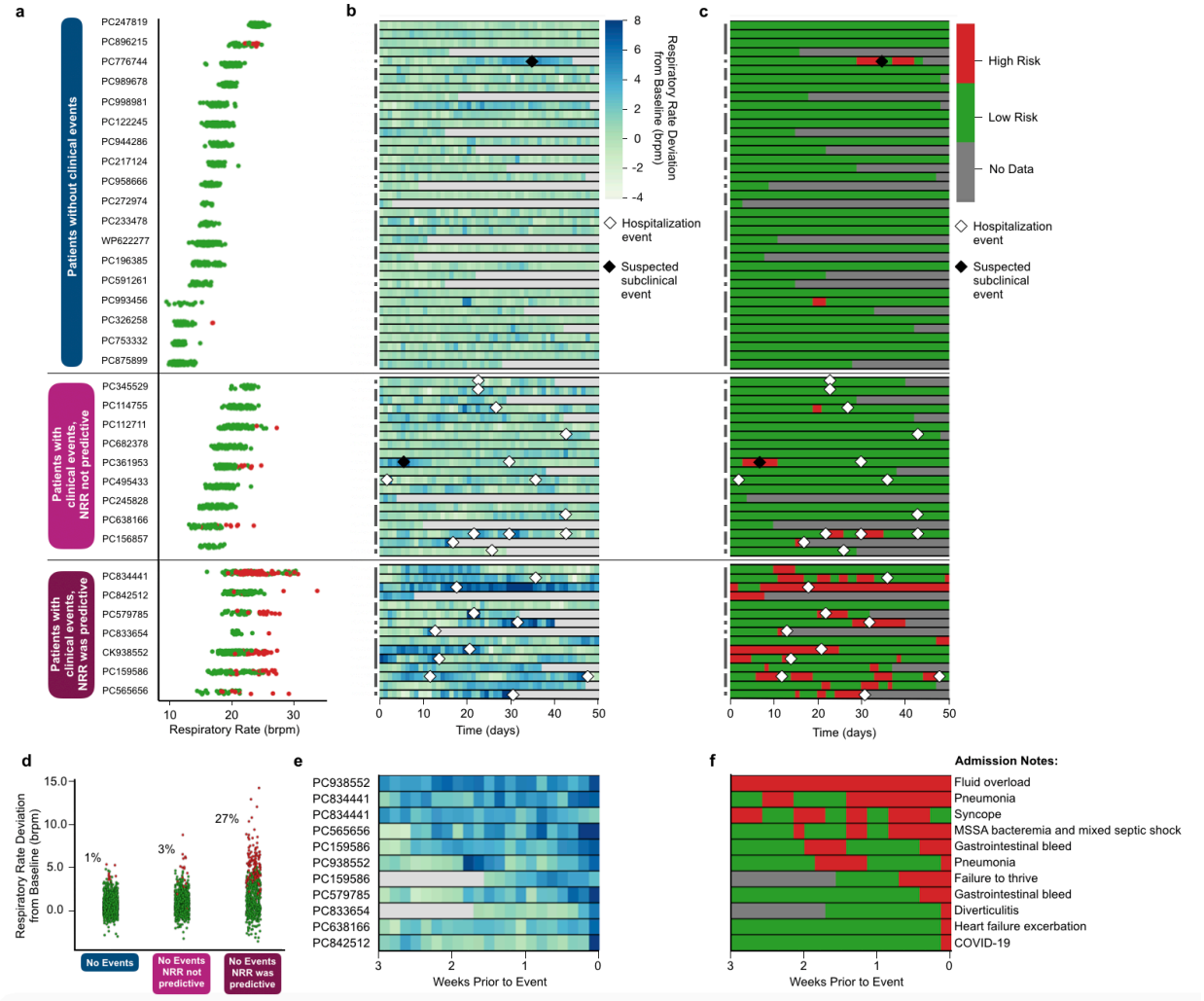

Figure 5-3. NRR and risk assessment for full data set. a, Dot plot of nocturnal respiratory rate for all nights of patient data, colored by low risk (green) and high risk (red). Patients are grouped into 3 categories, patients who had no clinical events (blue), patients who had clinical events but for whom NRR was not predictive (light magenta), and patients who had clinical events and for whom NRR was predictive (dark magenta). **b-c,** Heatmaps of respiratory rate deviation from baseline **(b)** and risk assessment **(c)** for all nights of patient data. Patients may span multiple rows. Gray used for padding. Hospitalization events annotated with white diamond. Suspected sub-clinical events annotated with gray diamond. Days with less than 3 hours of epochs not shown. **d,** Dot plot of NRR deviation from baseline for all patient-nights. Colored by low risk (green) and high risk (red) and grouped as described above. **e-f,** Heatmaps of NRR deviation from baseline **(e)** and risk assessment **(f)** for 3 weeks prior to hospitalization for events with respiratory rate prodromes. Days with less than 3 hours of epochs not shown. The same colorbars from **b-c** are used in **e-f**.

5.2 Discussion

Respiratory rate is a fundamental vital sign that is often clinically neglected, except at its extremes. Here, we show that NRR dynamics represents a powerful biomarker that can be passively monitored by non-contact sensors without requiring any patient engagement. Across 3400 patient-nights of longitudinal home bed monitoring in high-risk patients, we defined patterns of clinical stability and identified prodromes of impending hospitalizations for diverse causes. During periods of clinical stability, each patient exhibited low night-to-night variability compared to higher interpatient differences. This argued in favor of using patient-specific references rather than cross-sectional references. Doing so enabled early detection of respiratory changes days and weeks prior to hospitalization for conditions such as heart failure, diverticulitis, severe anemia due to gastrointestinal bleeding, pneumonia, acute COVID-19 infection, and septic shock.

Interpretation of impending hospitalizations using NRR is different from a molecular diagnostic test with a clear gold standard against which measurements can be compared and sensitivity and specificity quantified. There is no ground truth for acute and subacute illnesses or impending hospitalizations with respiratory prodromes. As expected, not all hospitalizations are preceded by respiratory prodromes. However, the inability to detect all causes of hospitalizations should not detract from those that can be detected. It is valuable to be able to detect clinical events days to weeks before patient-reported symptoms if it can be done without alarming on clinically stable or symptom-free patients. In our study, although we did alarm in a settings that did not result in hospitalizations, close examination of the associated NRR dynamics revealed that a subset exhibited rise-and-fall patterns suggestive of true subclinical

events for which outreach was desirable (Fig. C-5). In short, we propose a pragmatic approach to evaluation of NRR-based diagnostics – maximize detection of clinical events while minimizing alarms that have no clinical correlate when retrospectively evaluated.

Automated monitoring has potential to enable care coordinators to rapidly review large patient cohorts. Although events are automatically detected by the risk score algorithm, the data can be rapidly over-read for confirmation. Heatmaps place each day's data in the context of all prior days and web-based dashboards allow the automated results for each patient to be reviewed daily, requiring ~5 seconds per patient. This has the potential to substantially increase the number of patients a care coordinator can manage. Rather than performing randomly scheduled calls, time can be dedicated to those patients who are off their baseline and at risk of hospitalization. For example, consider a care coordinator who follows patients for 1-2 months after hospital discharge. At any given time, a care coordinator may be responsible for 100 high-risk patients with an average hospitalization rate of ~1 per year. Although the expected hospitalization rate is only 1 every few days, it is unknown which patients are off their baseline at any given time. Therefore, a commonly used strategy is to perform structured phone calls every few weeks. Contrast that with a workflow based on automated remote monitoring and NRR-prompted calls. A care coordinator could follow a substantially larger pool of patients with a similar risk profile (e.g., 1000 patients with 1 hospitalization per year). The automated alarm system is likely to surface 5-10 patients per day who are off their baseline at any given time. In addition to substantially expanding the number of patients a care coordinator can care for, it preserves time for calling patients and family members, performing home visits, and coordinating targeted examination, diagnostic testing, interventions, and follow-up when

necessary. In summary, the use of automated NRR-based early warning has potential to enable efficient allocation of care coordinator resources with minimal unwarranted alarms.

What is the appropriate intervention for a patient with impending hospitalization? Management of patients found to be off their baseline by in-home sensors is a largely unstructured domain of outpatient medicine that is likely to mature as providers are confronted with data from early detection technologies. The data should be viewed similarly to patient-reported symptoms rather than a result of a diagnostic lab test. It alerts the provider that the person is off their baseline, but additional conversation with or without objective diagnostic workup will be needed to define the way in which they are off their baseline. In our current workflow, early recognition of impending hospitalizations is communicated to care coordinators who call patients, discuss any symptoms, and if necessary, follow-up with additional phone calls, home visits, diagnostic tests, interventions, or escalation of care. Future work will prospectively test whether communicating NRR-informed risk scores to care coordinators, with or without accompanying structured workflows, can improve outcomes. This is particularly promising because many causes of increased NRR have established interventions. For more severe deteriorations, early evaluation in the ER and consideration of hospitalizations may reduce overall length of stays, need for ICU, or improve clinical outcomes after discharge. These questions will need to be tested prospectively to determine if NRR-guided care can improve the quality and cost of care as well as the quality of life for patients and their families.

5.3 Conclusion

In summary, we show that NRR, when monitored longitudinally using non-contact adherence-independent bed sensors, is a promising biomarker of impending hospitalizations. The potential for early recognition of acute and subacute illnesses makes outpatient chronic disease management a data-driven science and in doing so has potential to improve patient satisfaction and quality of care while reducing health care costs (48).

5.4 Methods

In this section, we describe in details the methods employed to acquire the results and generate the figures seen in the preceding sections.

5.4.1 In-home study

We started with a cohort of 41 in-home patients. We excluded patients who had less than 5 nights of data (impacting 6 patients) and we excluded an additional patient for technical reasons (see discussion of two-person issue below). Two patients (PC196385 and PC842512) had gaps in their records longer than 2 months and these regions were not included in our accounting of nights monitored or nights missed. Two patients (PC938552 and PC156895) had 5 nights with timing mismatch at the beginning of their records and these nights were not included. Two nights from PC345529 and PC989678 and 4 nights from PC217124 were excluded due to artifacts. Eight nights from PC245828 were excluded, 3 for artifacts, and 5 because, based on weight analysis, the data on those nights was not from our patient. Two patients (PC245828 and PC834441) had one set of sensors under their bed and another set of sensors under their recliner and these two data streams were combined to create a composite

record for each of them. The first 16 nights of PC233478 had a large proportion of artifacts and required a reinstall so we started their record after the reinstall. From the beginning to end of each patient's record there were 3,403 nights of data total and 3,056 nights with a sufficient number of epochs. On average, 91% of each patient's record contained nights with a sufficient number of epochs (Fig. C-2).

5.4.2 Two-person problem

Nine of our patients share a bed with a partner and so for these datasets there is uncertainty as to which individual is contributing to the NRR measurement from our sensor (one patient was excluded from our study due to this issue as it was clear that we were not monitoring our patient consistently). Of the 9 that were included, 1 patient (PC196385) was able to be partially isolated based upon weight and timing. Additionally, this patient had 2 hospitalization events that were successfully detected, indicating that this data set is matched to the correct person. For the remaining 8 patients we assumed that we are monitoring the correct individual and future work will employ two mattress sensors rather than BedScales (see Chapter 7) to disambiguate individuals who share a bed. Six of these 8 patients (PC217124, PC326258, PC753332, PC938552, PC944286, and PC989678) were not hospitalized which matches our NRR assessment as these individuals had almost entirely low risk nights. We acknowledge the possibility for false negatives for these patients if their data was reflective of the patient's partner and the partner was hospitalized for a disease exacerbation during our monitoring period. Two patients (PC361953 and PC682378) had events that went undetected by NRR and possibly these false positives were caused by this two-person issue.

5.4.3 Processing pipeline

To monitor the NRR, we used the BedScales platform described in Chapter 2. The processing pipeline used for the results in this Chapter are similar to that described previously. The resulting respiratory rate epochs from the pipelines were required to be within a physiologically reasonable range ($6<x<40$) and nights were required to contain at least 3 hours of epochs to be included. By convention, our "patient-nights" are defined as running from 12pm-12pm (changes due to daylight savings are not considered).

5.4.4 Clinical cohorts

Using the EMR, we recorded the significant interactions that our in-home patients had with clinicians. We separated the patients into a stable cohort (18 patients) and a hospitalized cohort (16 patients). We included in the hospitalized cohort all patients who were admitted overnight except for two patients (PC993456 and WP62227) because they were hospitalized for falls rather than a disease exacerbation. We included as an admission one patient (PC158695) who was admitted to a Skilled Nursing Facility. For correlating our in-home data with hospitalization events, standard calendar days were used and so events were recorded if they occurred up to midnight during the final night of monitoring for each individual.

5.4.5 Longitudinal in-home analysis

To assess the longitudinal stability of nocturnal respiratory rate for in-home patients (Fig. 5-1), we chose the patients who were not admitted to the hospital for a disease exacerbation and who had at least 30 nights of data, resulting in 480 nights total from 16 patients. The epochs for assessing stability were taken from a window of 30 nights that began at night 1 for these patients. For patients who had large gaps (>14 nights) of missing data during

this period, the 30-night window started after the gap period (this impacted patients PC196385 and PC217124). Variance comparison analysis was calculated using Levene test implemented by scipy.stats.levene.

5.4.6 Baseline calculation and self-referencing

To derive a baseline NRR for each patient, we found the causal moving average of each night with a window size of 5 nights and then took the rolling minimum of this value as it evolved across time. This ensured that each baseline value was the result of multiple nights of monitoring and that if our sensors were installed to a patient who was actively returning to their normal range, the derived baseline value would gradually decrease as the individual's respiratory rate returned to normal (Fig. C-3). Since there is no causal moving average defined for the first x-1 nights where x is the window size, when the baseline was subtracted from the nightly NRR estimate, all of the nights prior to a genuine baseline measure were set to a null value and not considered in subsequent analysis. A maximum of 1 night of missing data was allowed within the window of nights that was used in setting the moving average.

5.4.7 Clinically stable versus hospitalized patients

To see if there is any difference in NRR between clinically stable and hospitalized patients (Fig. 5-2e), we compared the distributions of baseline deviations across all nights for these two populations. To compare distributions comprised of nights near and far from hospitalization events (Fig. 5-2f), we defined a Proximity Factor that defined how many nights prior to the event were placed into the "near" distribution. To take into consideration that after the hospitalization event, the patient may be fully recovered, or may still be sick and recovering, we set a buffer value of 7 nights after the event and those nights were not placed into either the

“near” or “far” distributions. To compare the CDFs of the distributions in Figure 5-2, e-f, we used a Kolmogorov-Smirnov test for goodness of fit, implemented by scipy.stats.kstest.

For our risk assessment strategy, we set a threshold (RRth) that is a specified amount above baseline and in general, all nights above the threshold were considered high risk nights. To reduce noise from artifacts or from sporadic high-risk alerts, we incorporated 3 other considerations (Fig. C-4): (i) A night must either be the second consecutive above RRth to be considered high risk or (ii) the night must be above a higher threshold, RRth+ to be considered high risk. (iii) Nights that dropped below RRth could still be considered high risk if that night, and the other consecutive preceding high-risk nights (if any) had a mean that was still above the threshold. Considerations (i) and (ii) prevent sporadic or errant nights from being labeled high risk but allow for detection of acute conditions that suddenly raise the NRR (Fig. C-7c). Based on our dataset, we set RRth+ to be 1.75 brpm above RRth. Consideration (iii) is a causal way to prevent high risk regions from being fractured by nights that dip slightly below the threshold.

To count the number of events that were preceded by a rise in NRR (Fig. 5-2g), we set a margin value of 3, and any event that occurred within 3 nights of a high-risk night was considered to have been detected by NRR analysis. We set RRth based upon the value that would yield 1% or fewer high-risk nights in patients that were clinically stable (RRth99%). For our dataset, this value was 3.41 brpm.

5.4.8 Risk assessment

We applied our risk assessment strategy to the entire dataset (Fig. 5-3). We grouped patients into three categories (i) patients who had no hospitalization events (ii) patients who were hospitalized but for whom NRR was not predictive and (iii) patient who were hospitalized

and for whom NRR was predictive. To create the heatmaps in Figures 5-3, b-c we arranged all patient-nights in columns of 50 nights. Some patients spanned multiple rows and gray was used for padding to keep the columns even. Nights without data are not shown. We aligned all hospitalization events together and displayed 21 nights prior to each event (Fig. 5-3, 3-f). One patient in this figure, (PC842512) had their high-risk night on the same day as his admission so this was adjusted for display purposes.

5.5 Acknowledgements

Chapter 5 is largely a reprint of portions of material as it appears in the following manuscript prepared for submission: “Nocturnal Respiratory Rate Dynamics as Biomarkers of Impending Hospitalizations”, Harrington N, Barba DT, Bui Q, Wassell A, Khurana S, Rubarth RB, Sung K, Owens RL, Agnihotri P, King KR. The dissertation author was the primary investigator and author of this paper.

Chapter 6: Case Studies

In this Chapter, we present three case studies of specific patients. These clinical cases highlight the ability of adherence independent monitoring to track NRR changes prior to a hospitalization event and demonstrate in real-world scenarios the potential benefit of home monitoring as a means of improving outpatient care.

Section 6.1 Failure to thrive

Our first case study involves a patient who had two hospitalizations during our initial monitoring period, as seen in the heatmap in Figure 6-1 below. The first clinical event occurred around the second week of monitoring. The patient was found to have a hemoglobin count of 6.2 and was referred to the emergency department. Upon examination, he was admitted overnight to the hospital for a gastrointestinal bleed and underwent EGD. There is a clear rise and fall of NRR prior and post this admission. The NRR then rose again, starting around week five, prompting a home visit by a nurse. The nurse evaluated the patient and due to his inability to complete activities of daily living, he was admitted to a skilled nursing facility. This case shows the ability of NRR to warn of an impending clinical event. Additionally, this case highlights the wide variety of events that can cause a rise of NRR as here the issues were more related to quality of life and pain than they were to a specific pulmonary based infection or decompensation.

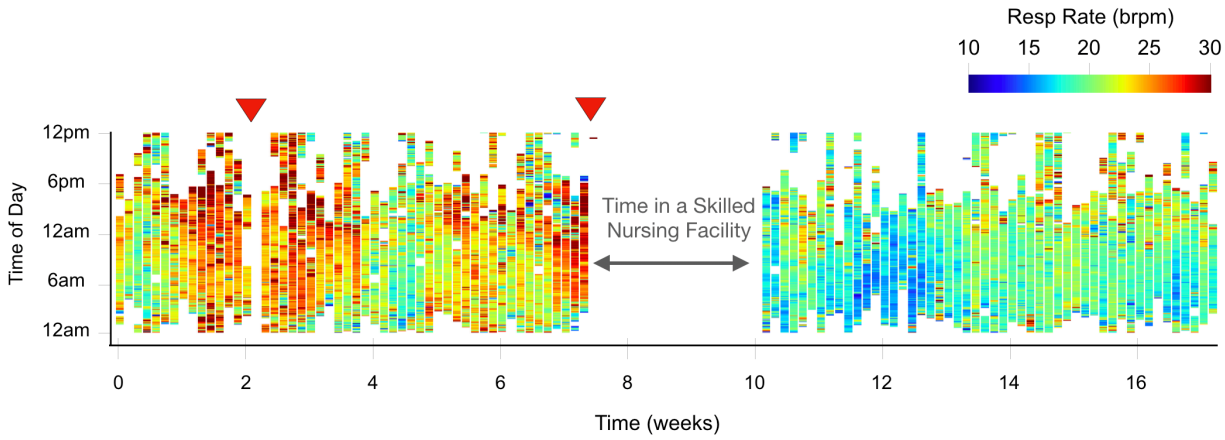

Figure 6-1. Nocturnal respiratory rates prior to admissions. Heatmap of NRR measured in breaths per minute (brpm) by BedScales. Color range from 10 to 30 brpm, rates below 10 not shown. Red arrows show days of admissions. Respiratory rates increase prior to each admission and return to a lower level after time in skilled nursing facility.

6.2 Development of sepsis

The second case study involves a patient who acquired sepsis (the systemic response to infection) resulting in a multi-week hospitalization. The patient was an 85-year-old African American woman who lived alone, was legally blind and morbidly obese. Additionally, she had multiple comorbidities including end-stage renal disease and ischemic cardiomyopathy with recurrent heart failure hospitalizations (ejection fraction 15%). As part of our observational study (described in Chapter 5), NRR was longitudinally monitored in her home bed using our BedScales platform (described in Chapter 2). Figure 6-2 shows the patient's NRR for 1 month prior to her septic shock hospitalization. Baseline nocturnal respiratory rates of 14-18 breaths per minute increased during the 48 hours prior to hospitalization reaching sustained rates above 25 and 30 breaths per minute.

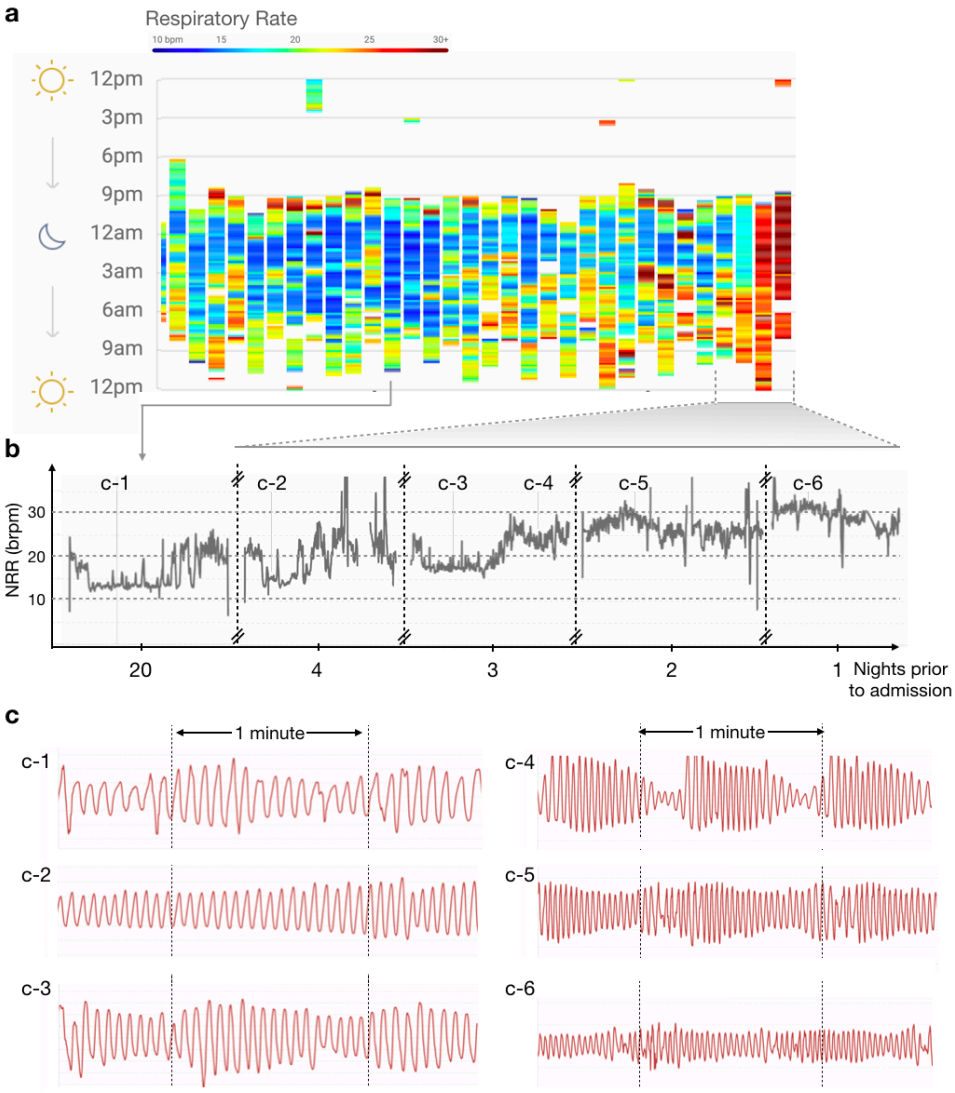

Figure 6-2. Nocturnal respiratory rates during emergence of septic shock in the home. a, Heatmap of NRR 1 month prior to admission for septic shock. **b,** Respiratory rates (NRR) shown across time at 20 days prior to admission (c-1) and for each of the 4 days prior to admission (c-2-c-6). Hashes indicate discontinuities in the time axis. **c,** Examples respiratory waveforms measured by the bed sensor are shown at the numbered locations in (b).

Sepsis is a common, costly, and frequently fatal condition thus the ability to detect sepsis in the home is very important because mortality due to sepsis increases with each hour that antimicrobial therapy is delayed (49)(50). This has fueled campaigns to improve early recognition of sepsis, but these have primarily focused on clinical settings such as the emergency room and hospital (50). This case suggests that adherence-independent home

monitoring of NRR may extend the sepsis recognition window by hours to days. Doing so could facilitate expedited evaluation and early initiation of antimicrobial therapy to reduce sepsis-associated morbidity and mortality.

Section 6.3 Acute pulmonary embolism

Our final case study involves a patient whose heatmap can be seen in Figure 6-3 below. The patient's steady increase in NRR across time prompted two phone calls to the patient's home (on days eight and four prior to admission) during both of which no acute symptomatic changes were noted. However, the NRR worsened following the second call. The next evening the NRR steadily improved but a visiting nurse arrived on the day of admission and found the patient subjectively dyspneic, tachypneic in the high 20s, and hypoxic with an oxygen saturation of 80s. Patient was transferred to the emergency department and it was found that she had a pulmonary embolism. She was started on anticoagulation and hospitalized. During the admission she underwent additional dieresis to treat volume overload. Through the lens of the NRR heatmap, there is a marked improvement once she returns home from her admission.

This example is important because acute pulmonary embolisms are unheralded events associated with cancer, immobility, and inherited conditions that can be fatal if not treated with anticoagulation. Many acute pulmonary embolisms develop outside of clinical settings, and here we show the ability of the BedScales platform and NRR to detect a pulmonary embolism, and in this case, actually impact the patient's care.

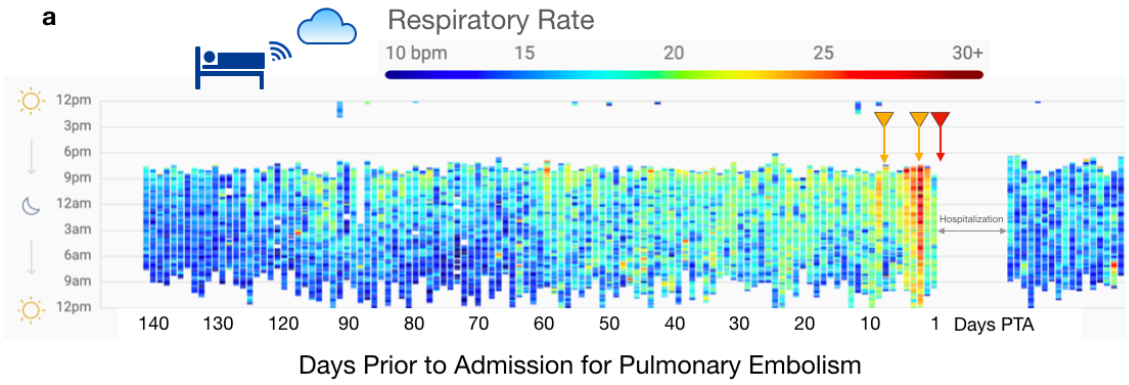

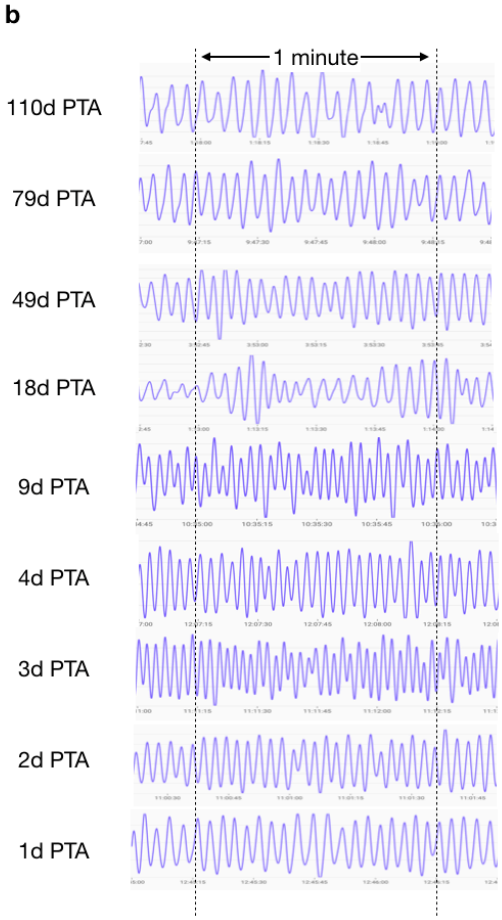

Figure 6-3. Nocturnal respiratory rates prior to admission for pulmonary embolism. a, A heatmap of nocturnal respiratory rates measured in breaths per minute (brpm) by a non-contact adherence-independent home bed sensor for over three months during which the patient developed worsening tachypnea over 5 days before presenting to the emergency department. Orange arrows show days on which the patient's home was called. Red arrow shows day of admission. **b,** Respiratory waveform tracings shown on 9 different days spanning from 110d-1d prior to admission (PTA).

6.4 Acknowledgements

Chapter 6 contains portions of material as it appears in the following manuscripts prepared for submission: “Development of sepsis in the home bed”, Harrington N, Agnihotri P, King KR. The dissertation author was the primary investigator and author of this paper. “Development of an acute pulmonary embolism in the home bed”, Barba DT, Harrington N, Agnihotri P, King KR. The dissertation author was the secondary author of this paper.

Chapter 7: Future Work and Conclusion

In this chapter I will close by reflected on future work required and then summarizing our results. As described in the section 6.3, we initiated a clinic visit for a patient who had a previously unknown pulmonary embolism. However, what is unique about that case is that that patient was using a mattress sensor (Emfit, Finland), rather than our BedScales platform. This shows that the pipeline and analytics that we developed is sensor agnostic. This is important because for future work, we will be exploring the use of other sensors that have much lower requirements for installation. The BedScales platform's key limitation is that it is difficult to install, as the bed must be lifted or dissembled in order to place the scales underneath the legs. The initial motivation to require such an arduous installation was to be able to measure total body weight, but as described at the end of Chapter 3, more work will need to be down to facilitate such measurements automatically in real-world settings. We therefore have pivoted to using standard mattress sensors, after discovering that NRR was much more powerful than previously expected and that it alone can provide insight into impending hospitalizations.

In conclusion, our goal was to provide clinicians with advanced warning of disease decompensation. To do this, we set out to measure clinically useful biomarkers and to create a system that is pragmatically applicable. We have sought to ensure that this device will be used by patients, by designing it to be adherence independent, low-cost, and durable. Additionally, we have been sensitive to the needs of clinicians and designed a system that will not overload them with difficult to interpret data, but that provides clear pictures of patient health (heatmaps) and a risk score of NRR elevations. We have shown that NRR is a previously overlooked yet

very useful biomarker. We have analyzed it in populations and have monitored it longitudinally in a non-contact adherence independent manner. We have observed numerous hospitalizations, for a variety of diseases, where NRR rose prior to admission, sometimes even weeks in advance. We believe that this work serves to advance our ability to care for patients in-home and will both improve patient quality of life as well as lower costs.

Appendix A: Supplement for Chapter 3

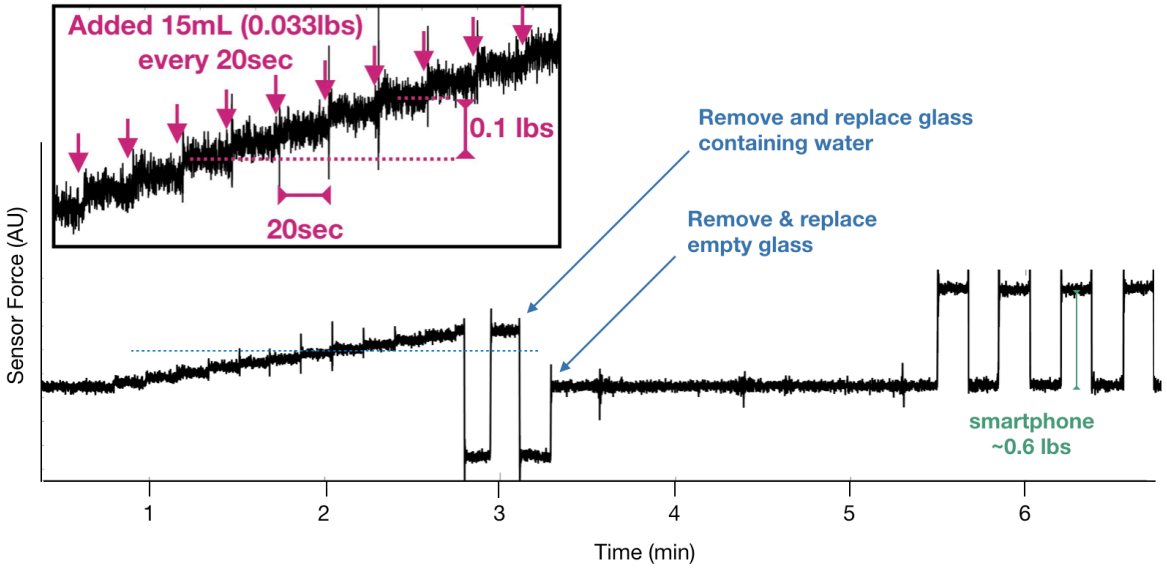

Figure A-1. Demonstration of BedScales weight sensor sensitivity. 15ml of water were added every 20 seconds to demonstrate signal-to-noise ratio of sensor.

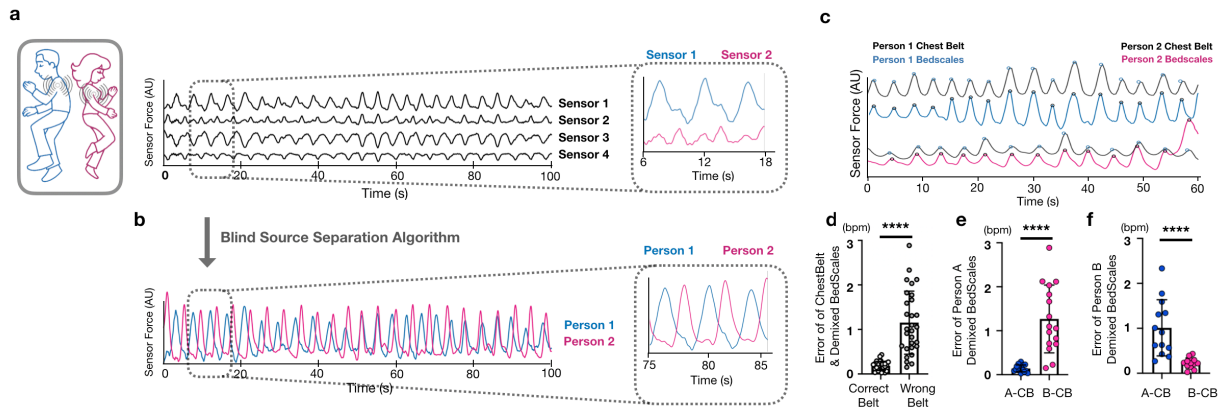

Figure A-2. Strategy for separation of respiratory signals when two persons share the bed. a, Cartoon illustrating how two persons sharing a bed are modeled as two respiratory point sources and raw signals from the 4 legs of the bed beneath two sleeping individuals. Inset shows 2 sensors each predominantly measuring one person with contaminating signal from the second person. **b,** Demixed signals for person 1 (blue) and person 2 (pink) derived from the raw signals in A. **c,** Validation experiment comparing demixed BedScales signals (blue and pink) with the corresponding ground truth chest belt signals (black). **d,** Bar plot comparing peak location errors across both subjects between the demixed signal and the "correct chest belt "versus the error between the demixed signal and the "wrong chest belt." **e-f,** Bar plot quantifying the error between the BedScales separated signal from subject A **(e)** or B **(f)** and the chest belt on subject A (A-CB, left) or subject B (B-CB, right). Data are shown as mean ± standard deviation. ****P < 0.0001, Mann–Whitney test.

Demixing of respiratory signals obtained from two simultaneous sleepers was performed using a hidden Markov model. Mechanical respiratory sources were interpreted as latent signals that evolve in a stochastically continuous manner, according to a linear additive Gaussian model, mixed through a linear operation with additive sensor noise to give rise to the signals at the four detectors. Interpreting the linear operation as unknown, we used the Expectation–Maximization algorithm to obtain the maximum-likelihood estimate (51). Given this estimate, the Kalman smoothing algorithm was used to extract the mechanical respiratory patterns of the two sources (52). Validation was performed by simultaneously but independently measuring each respiratory signal using two respiratory belts (Vernier, Beaverton, OR). Interbreath intervals were compared by measuring the error between each demixed signal and each ground truth respiratory belt signal. For each individual, the absolute error between the putative demixed source signal and each respiratory belt signal was calculated and compared using a t test.

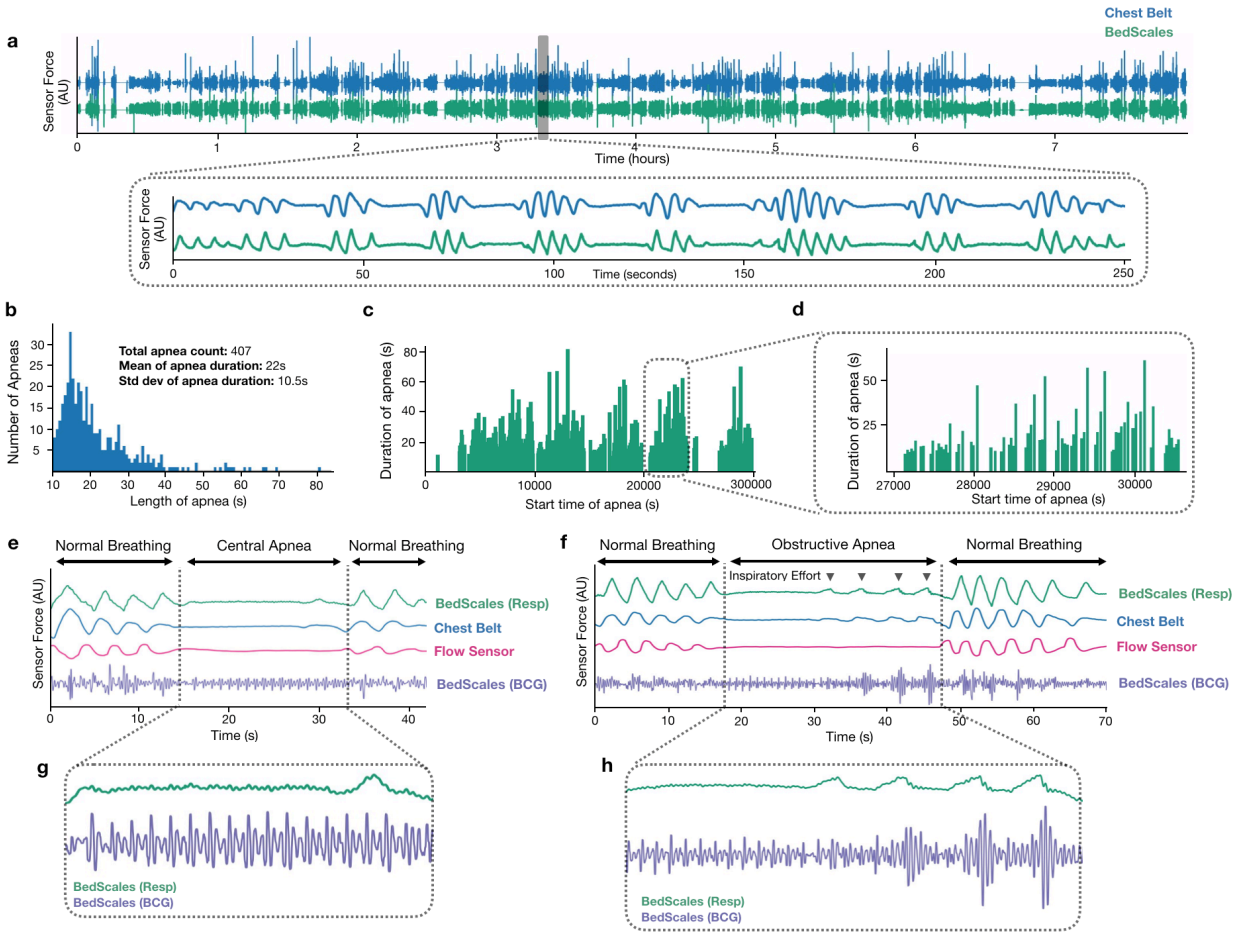

Figure A-3. Example patient with mixed obstructive and central sleep apnea during simultaneous sleep study and BedScales monitoring. a, BedScales non-contact respiratory signal (green) compared to chest respiratory belt (blue) during overnight sleep study. Inset illustrates the overnight burden of apneas. **b,** Histogram of all apneas. **c,** Duration of apneas vs timing of apneas throughout the overnight study. **d,** High temporal resolution from one of the five apnea clusters during the night. **e,** Central sleep apnea episode and **f,** obstructive sleep apnea episode comparing BedScales respiratory signal (green) with chest belt (blue), nasal flow sensor (pink) and BedScales BCG (purple). **g-h,** Insets show detailed BedScales respiratory and BCG signals during a (**g**) central apnea (no respiratory effort) and (**h**) an obstructive apnea (low amplitude respiratory effort against a closed airway).

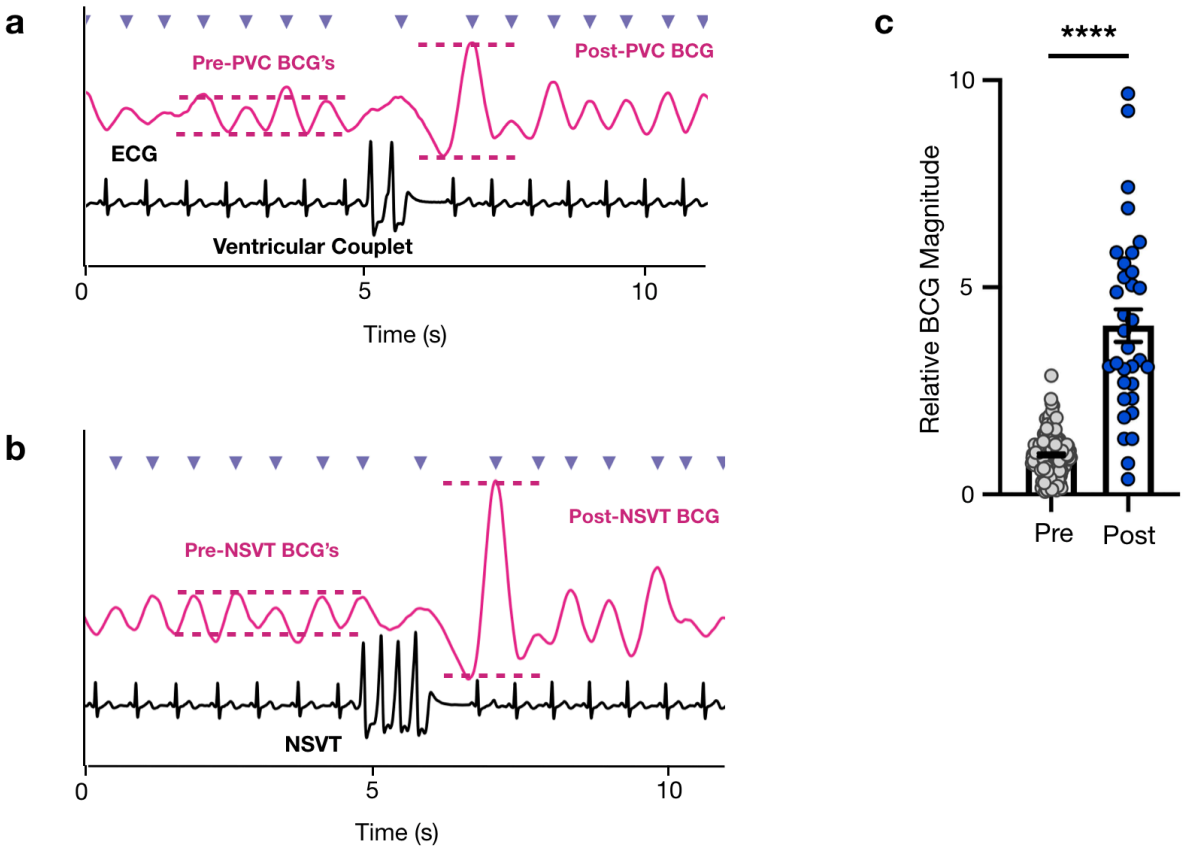

Figure A-4. Hemodynamic consequences of arrhythmias. a, Single-peak BCG (pink) compared to ECG (black) with peak annotation (purple arrows) surrounding a ventricular couplet. Pink annotations highlight the BCG magnitude increase after the ventricular couplet. **b,** Single-peak BCG (pink) compared to ECG (black) with peak annotation (purple arrows) during a region of non-sustained ventricular tachycardia (NSVT). Pink annotations highlight the BCG magnitude increase surrounding the NSVT. **c,** Bar plot quantifying the relative magnitude of BCG beats occurring before ventricular couplets, triplets or NSVTs (gray) compared to the BCG beat immediately following the ectopy (blue). Data are shown as mean ± standard deviation. ****$P < 0.0001$, Mann–Whitney test.

Appendix B: Supplement for Chapter 4

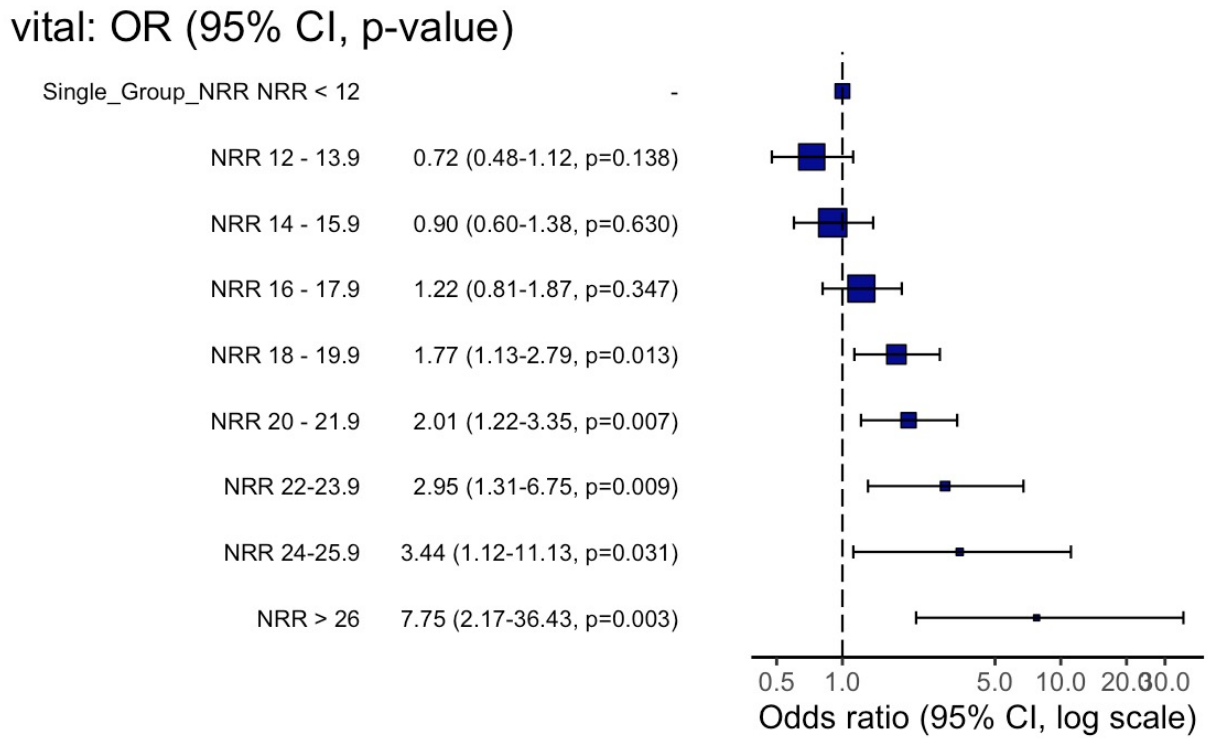

Figure B-1. Odd ratio linking NRR to outcomes in SHHS study. A granular analysis across different NRR subgroups reveals an increasing association (odds ratio) between NRR and mortality; this is particularly true for NRR rates at 18 bpm and above, where all associations appear to be statistically significant ($p<0.05$) and with increasing odds ratios and 95% CI ranges.

Appendix C: Supplement for Chapter 5

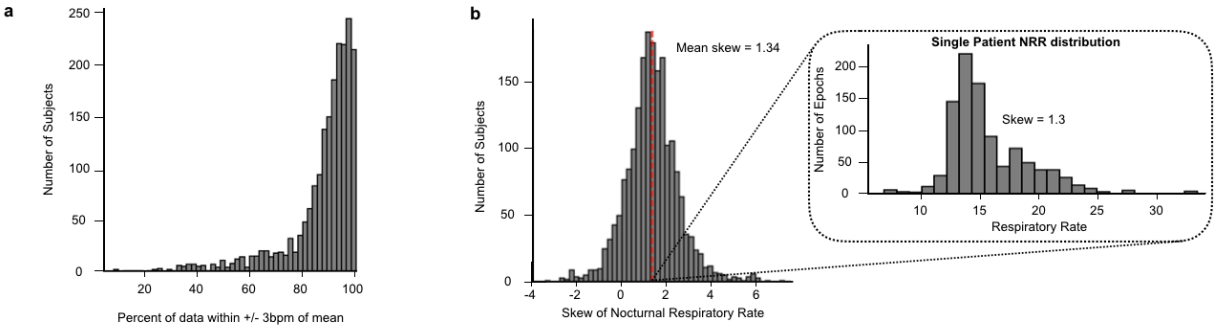

Figure C-1. Nocturnal respiratory rate sleep study intra-night statistics. a, Histogram of percent of respiratory rates within 3 brpm of each sleep study subject's mean. **b,** Histogram of skew per sleep study subject. Red dashed line indicates mean of skew (1.33). Inset show nocturnal respiratory rate distribution for a patient with a typical skew value (1.3).

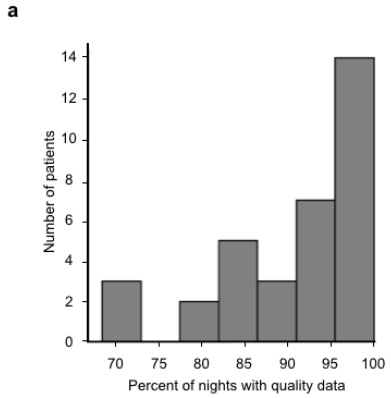

Figure C-2. Percent of nights with sufficient data. a, Histogram of percent of nights within monitoring period that contained at least 3 hours of quality epochs.

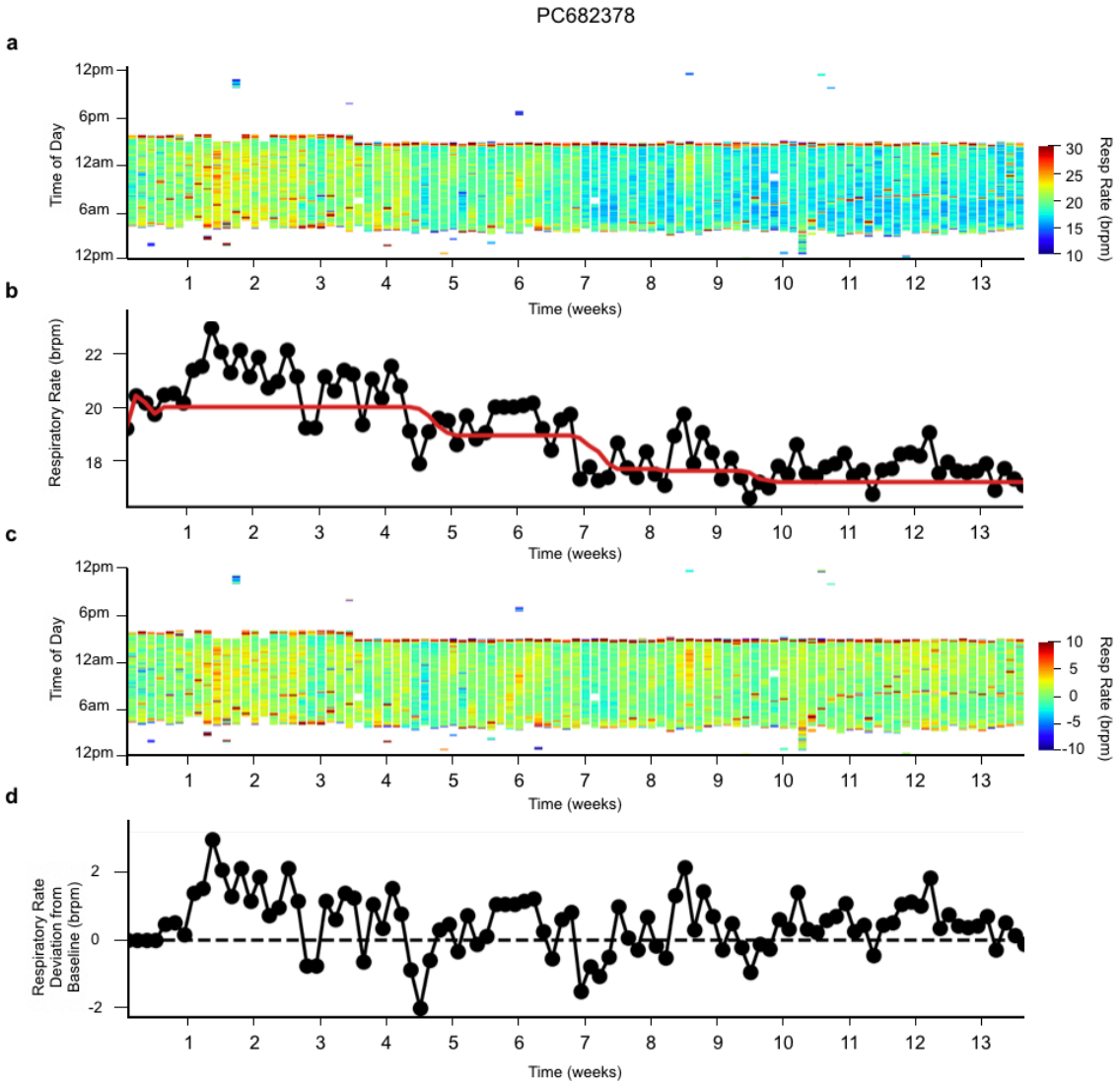

Figure C-3. Causal adaptive baseline correction. a, Heatmap of NRR for a patient with a monotonically decreasing brpm. Colorbar ranges from 10-30 brpm, values below 10 brpm not shown. **b,** Nightly median respiratory rate (black) with causal baseline annotated (red). **c,** Heatmap of NRR with baseline subtracted. Colorbar ranges from -10 to 10 brpm, values below -10 not shown. **d,** Nightly median respiratory rate (black) with baseline subtracted.

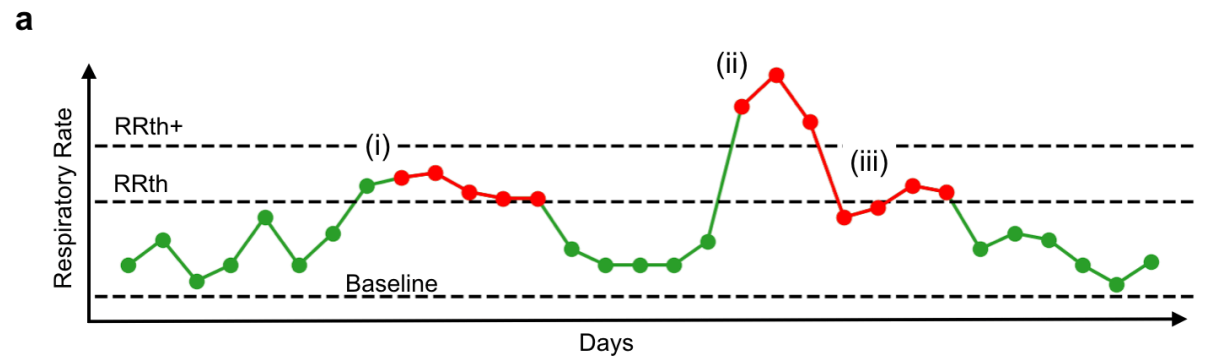

Figure C-4. Risk assessment strategy. a, Illustration of risk inference from NRR dynamics. Respiratory rates are plotted across time colored by low risk (green) and high risk (red). Horizontal dashed lines indicate the baseline NRR, the NRR threshold (RR_{th}) and the additional NRR threshold (NRR+). In general, points below the first threshold (RR_{th}) are low risk and points above are high risk. Roman numerals highlight regions of special consideration (see Methods). **(i)** Demonstrates that nights above the first threshold are only considered high risk if they are the second consecutive point above the threshold. **(ii)** Demonstrates that if a night is above the second threshold (NRR+) it is always considered high risk. **(iii)** Demonstrates that nights below the first threshold are still considered high risk if the days preceding them have an overall mean that is above the first threshold.

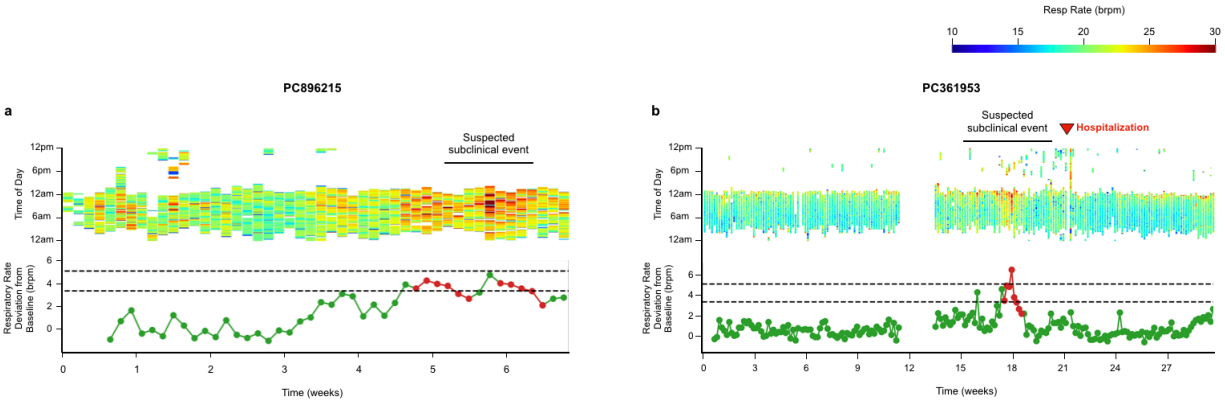

Figure C-5. Suspected subclinical events. Heatmap and corresponding NRR deviation from baseline for two patients who both exhibited a steady rise and fall of brpm indicative of a disease exacerbation. Heatmap colorbar ranges from 10-30 brpm, values below 10 brpm not shown. NRR excursions colored by low risk (green) and high risk (red). Black dashed lines show RRth (bottom) and RRth+ (top). PC896215 (a) was never seen in clinic during our monitoring period and PC361953 (b) was seen in clinic for orthostatic hypotension 3 weeks after the suspected subclinical event was resolved.

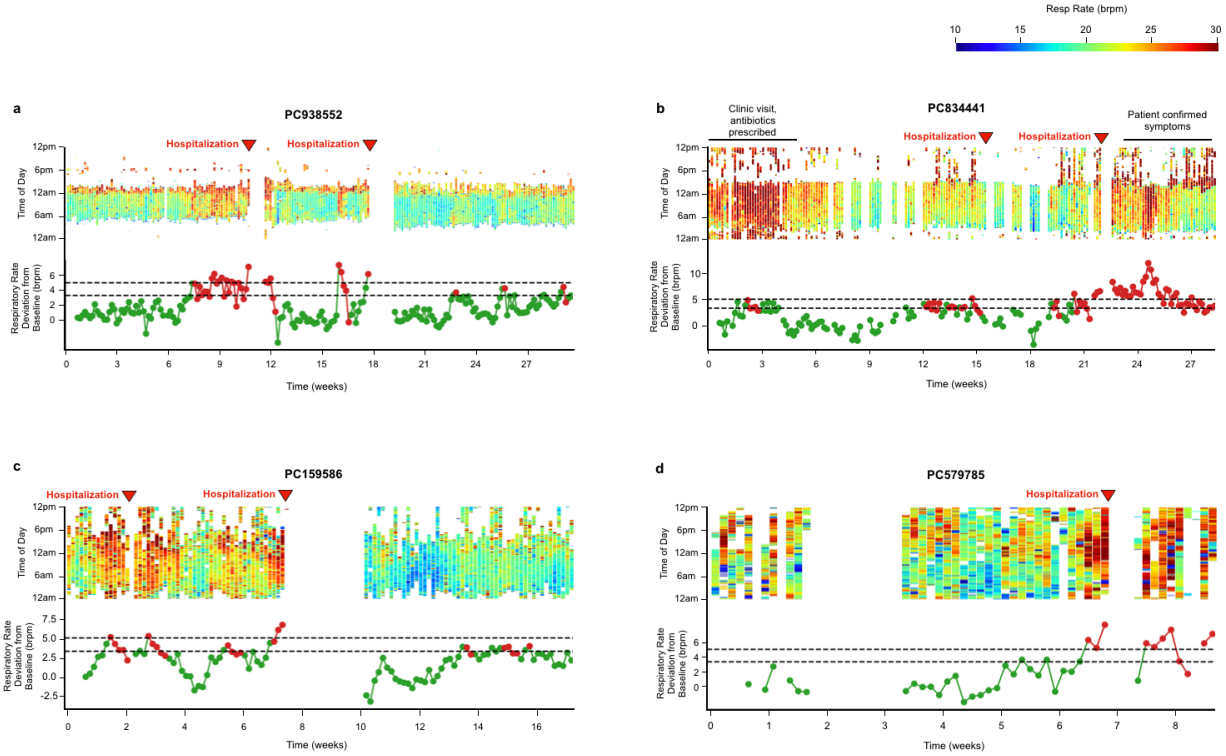

Figure C-6. Heatmaps for patients with clinical events, NRR predictive. Heatmap and corresponding NRR deviation from baseline for 4 patients whose events were preceded by a rise in NRR. Heatmap colorbar ranges from 10-30 brpm, values below 10 brpm not shown. NRR excursions colored by low risk (green) and high risk (red). Black dashed lines show RRth (bottom) and RRth+ (top). **a,** Patient had two hospitalization events, the first for fluid overload (+/- pneumonia), the second for pneumonia and mild fluid overload. **b,** Patient had two hospitalization events, the first for syncope, the second for pneumonia and mild fluid overload. **c,** Patient had two clinical events, the first was a hospitalization for a gastrointestinal bleed, the second was a referral to a skilled nursing facility for failure to thrive (inability to complete ADLS and for knee pain). **d,** Patient was hospitalized due to concern for gastrointestinal bleed.

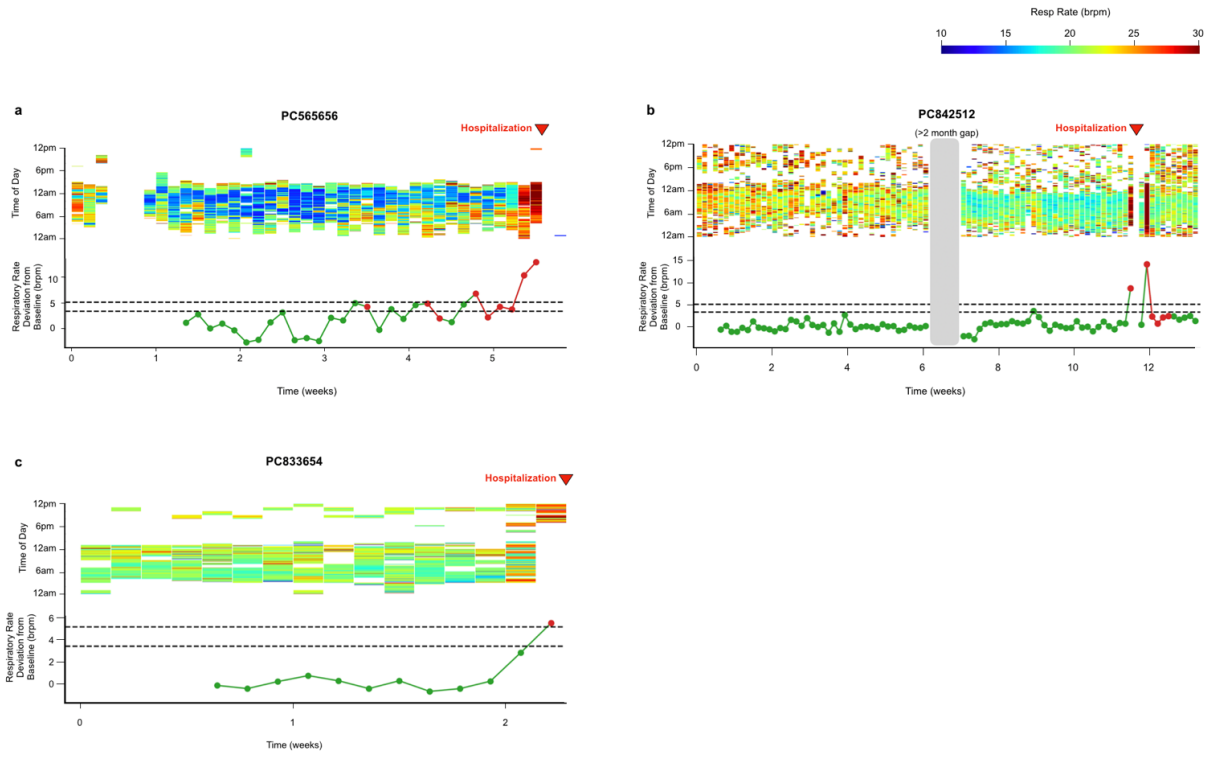

Figure C-7. Heatmaps for patients with hospitalization events, NRR predictive. Heatmap and corresponding NRR deviation from baseline for 3 patients whose events were preceded by a rise in NRR. Heatmap colorbar ranges from 10-30 brpm, values below 10 brpm not shown. NRR excursions colored by low risk (green) and high risk (red). Black dashed lines show RRth (bottom) and RRth+ (top). **a,** Patient was referred to emergency department for shortness of breath and difficulty walking. Was admitted for MSSA bacteremia and mixed septic shock. **b,** Patient was hospitalized for fever and chills. Was found to have COVID-19. **c,** Patient was seen in emergency department for altered mental status and malaise. Was hospitalized for diverticulitis.

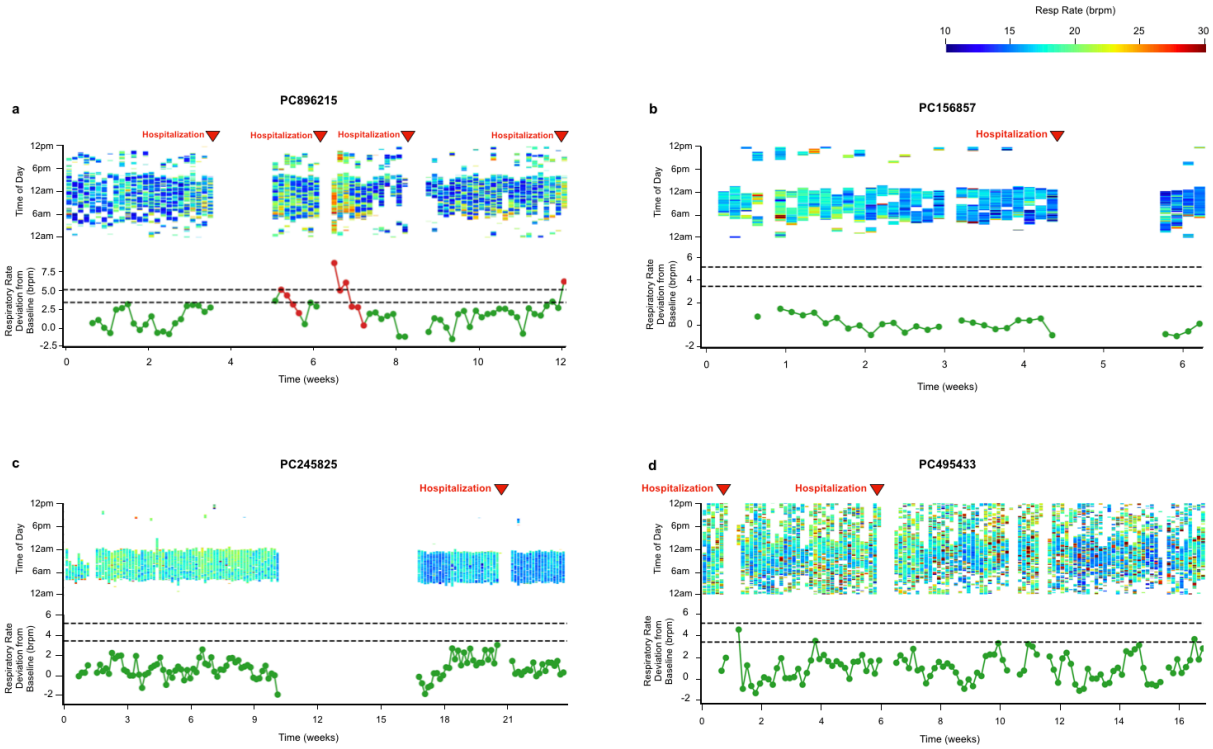

Figure C-8. Heatmaps for patients with hospitalization events, NRR not predictive. Heatmap and corresponding NRR deviation from baseline for 4 patients whose hospitalization events were not preceded by a rise in NRR. Heatmap colorbar ranges from 10-30 brpm, values below 10 brpm not shown. NRR excursions colored by low risk (green) and high risk (red). Black dashed lines show RRth (bottom) and RRth+ (top). **a,** Patient had 4 hospitalization events, the first for volume overload, the second for symptomatic bigeminy and ectopy, the third for cellulitis, and the fourth for heart failure exacerbation (this event was associated with a rise in NRR). **b,** Patient was referred for cellulitis symptoms, was found to have heart failure. **c,** Patient was hospitalized for congestive heart failure exacerbation. **d,** Patient had two hospitalization events, the first for over-diuresis, the second for hyperglycemia and hypovolemia.

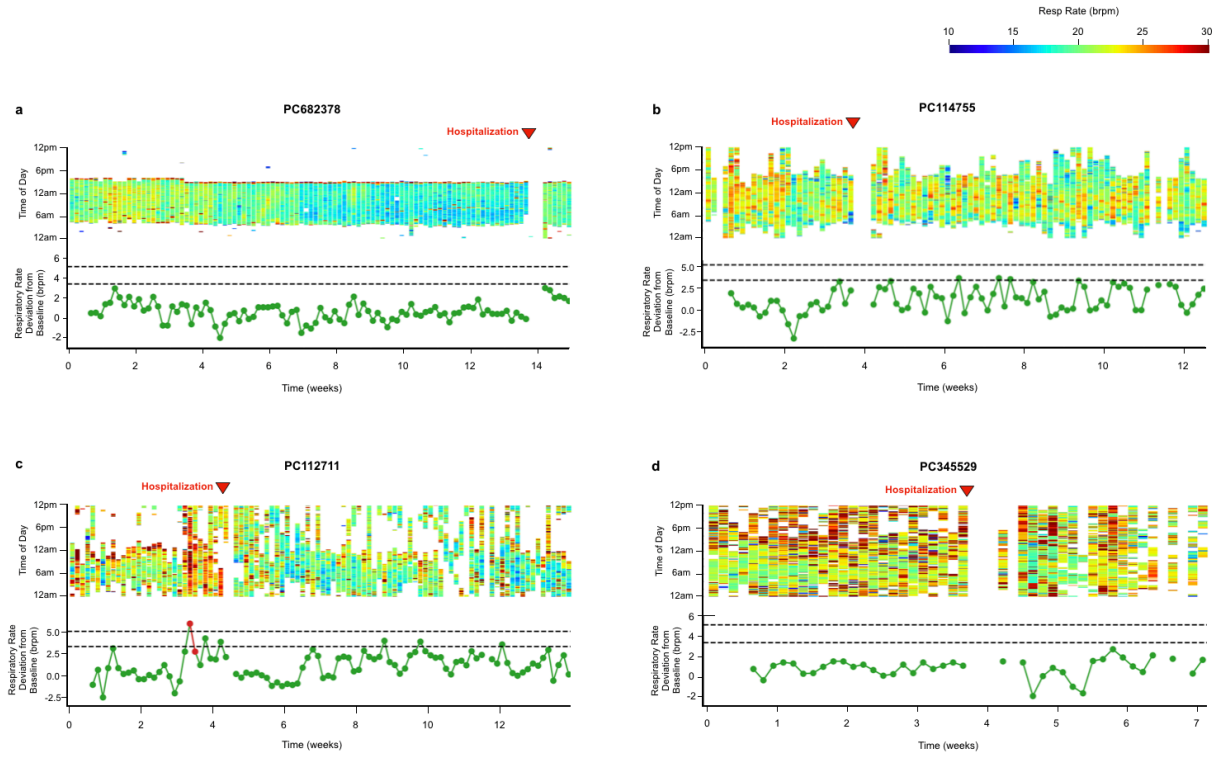

Figure C-9. Heatmaps for patients with hospitalization events, NRR not predictive. Heatmap and corresponding NRR deviation from baseline for 4 patients whose hospitalization events were not preceded by a rise in NRR. Heatmap colorbar ranges from 10-30 brpm, values below 10 brpm not shown. NRR excursions colored by low risk (green) and high risk (red). Black dashed lines show RRth (bottom) and RRth+ (top). **a,** Patient was hospitalized for hypoglycemia. **b,** Patient was hospitalized for atrial flutter. **c,** Patient was hospitalized for COVID-19. **d,** Patient was hospitalized for volume overload.

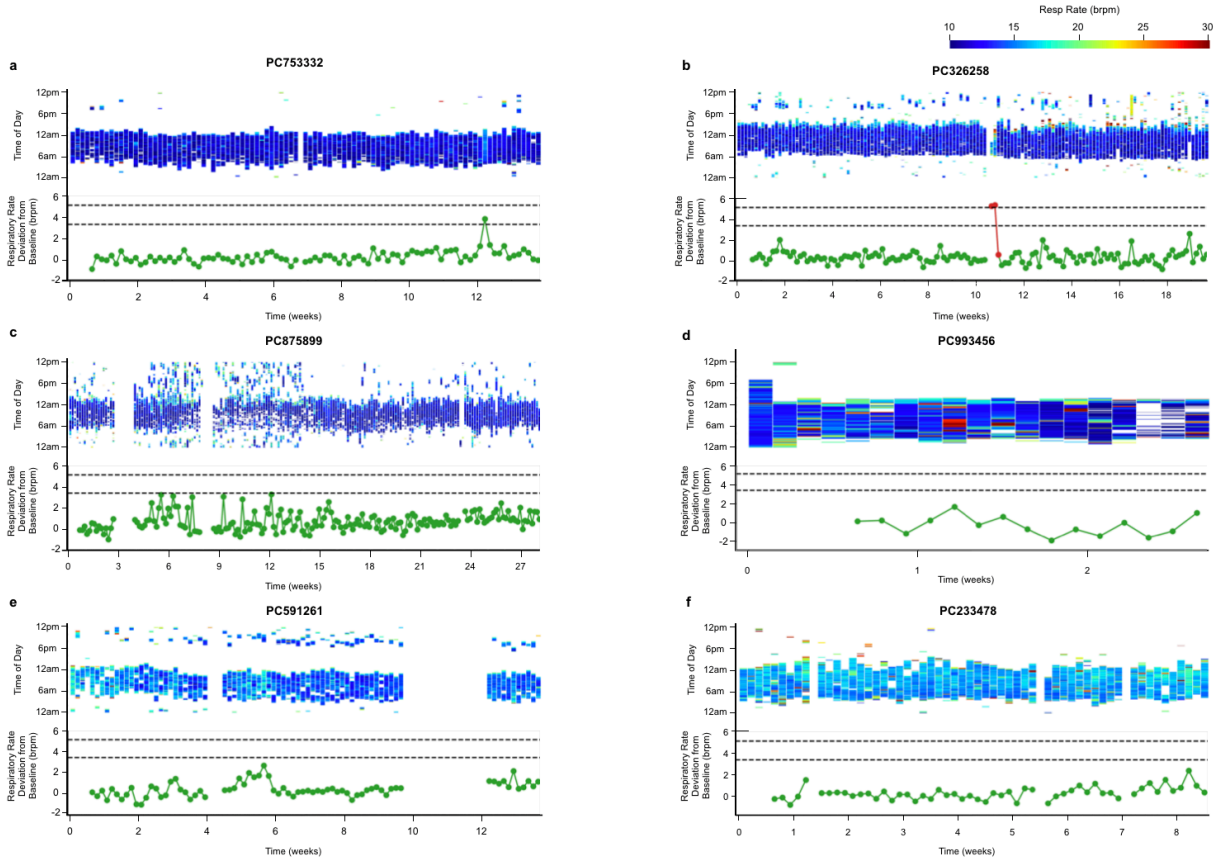

Figure C-10. Heatmaps for patients without hospitalization events. Heatmap and corresponding NRR deviation from baseline for 6 patients who did not have hospitalization events during our monitoring period. Heatmap colorbar ranges from 10-30 brpm, values below 10 brpm not shown. NRR excursions colored by low risk (green) and high risk (red). Black dashed lines show RRth (bottom) and RRth+ (top).

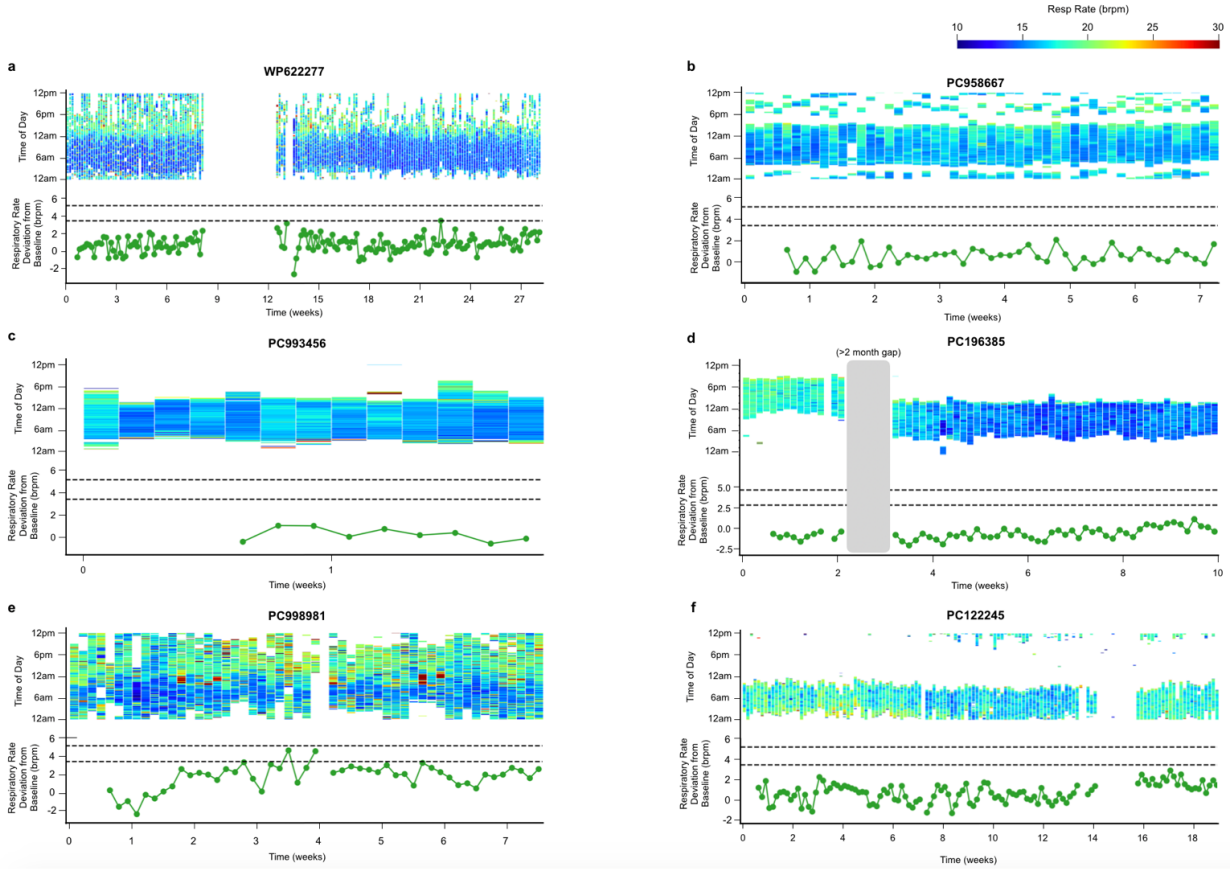

Figure C-11. Heatmaps for patients without hospitalization events. Heatmap and corresponding NRR deviation from baseline for 6 patients who did not have hospitalization events during our monitoring period. Heatmap colorbar ranges from 10-30 brpm, values below 10 brpm not shown. NRR excursions colored by low risk (green) and high risk (red). Black dashed lines show RRth (bottom) and RRth+ (top).

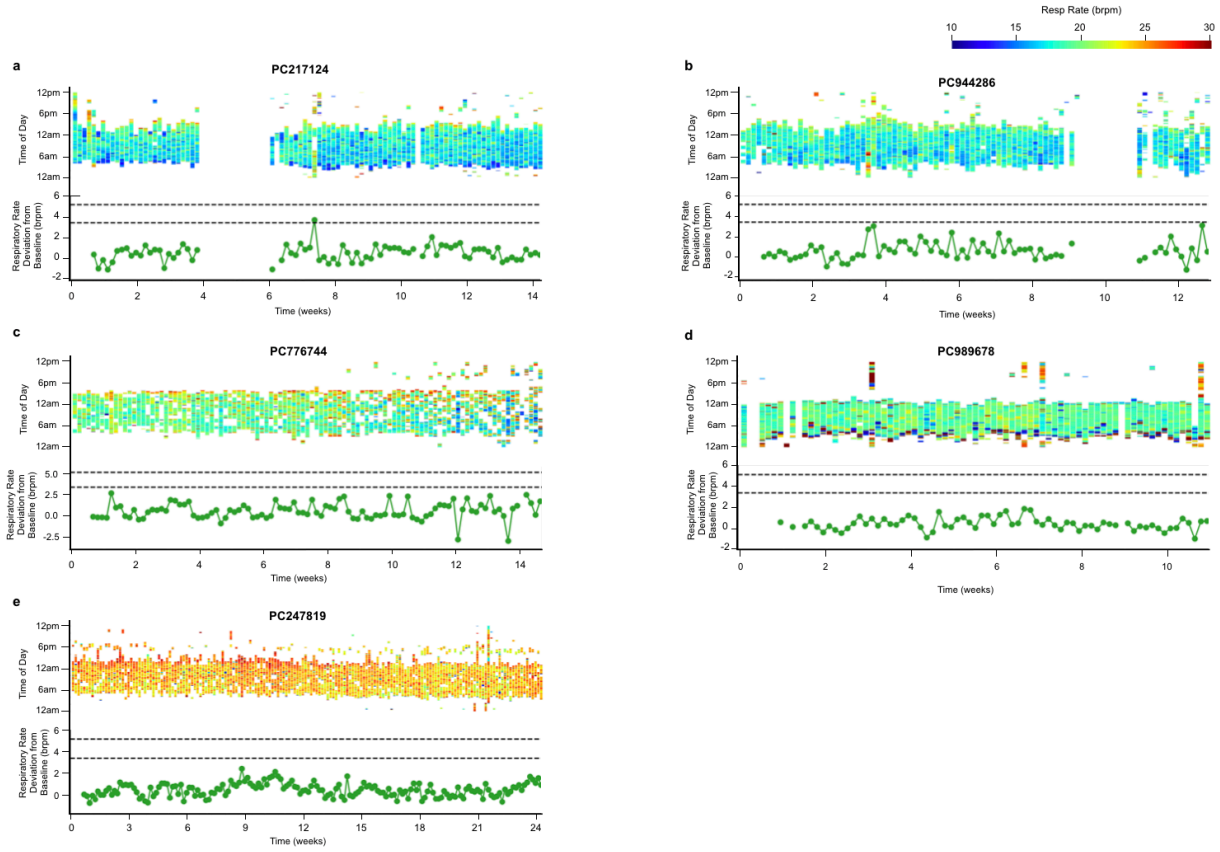

Figure C-12. Heatmaps for patients without hospitalization events. Heatmap and corresponding NRR deviation from baseline for 5 patients who did not have hospitalization events during our monitoring period. Heatmap colorbar ranges from 10-30 brpm, values below 10 brpm not shown. NRR excursions colored by low risk (green) and high risk (red). Black dashed lines show RRth (bottom) and RRth+ (top).

References

1. Heidenreich, P. A., Albert, N. M., Allen, L. A., Bluemke, D. A., Butler, J., Fonarow, G. C., Ikonomidis, J. S., Khavjou, O., Konstam, M. A., Maddox, T. M., Nichol, G., Pham, M., Piña, I. L., Trogdon, J. G., American Heart Association Advocacy Coordinating Committee, Council on Arteriosclerosis, Thrombosis and Vascular Biology, Council on Cardiovascular Radiology and Intervention, Council on Clinical Cardiology, Council on Epidemiology and Prevention, & Stroke Council (2013). Forecasting the impact of heart failure in the United States: a policy statement from the American Heart Association. *Circulation. Heart failure*, *6*(3), 606–619.

2. van Walraven, C., Bennett, C., Jennings, A., Austin, P. C., & Forster, A. J. (2011). Proportion of hospital readmissions deemed avoidable: a systematic review. *CMAJ : Canadian Medical Association journal = journal de l'Association medicale canadienne*, *183*(7), E391–E402.

3. Desai, A. S., & Stevenson, L. W. (2012). Rehospitalization for heart failure: predict or prevent?. *Circulation*, *126*(4), 501–506.

4. Planinc, I., Milicic, D., & Cikes, M. (2020). Telemonitoring in Heart Failure Management. *Cardiac failure review*, *6*, e06.

5. Reza, N., DeFilippis, E. M., & Jessup, M. (2020). Secondary Impact of the COVID-19 Pandemic on Patients With Heart Failure. *Circ Heart Fail* 13, e007219

6. Buchman, T. G., Simpson, S. Q., Sciarretta, K. L., Finne, K. P., Sowers, N., Collier, M., Chavan, S., Oke, I., Pennini, M. E., Santhosh, A., Wax, M., Woodbury, R., Chu, S., Merkeley, T. G., Disbrow, G. L., Bright, R. A., MaCurdy, T. E., & Kelman, J. A. (2020). Sepsis Among Medicare Beneficiaries: 1. The Burdens of Sepsis, 2012-2018. *Critical care medicine*, *48*(3), 276–288.

7. Wallace, A. E., Kaila, S., Bayer, V., Shaikh, A., Shinde, M. U., Willey, V. J., Napier, M. B., & Singer, J. R. (2019). Health Care Resource Utilization and Exacerbation Rates in Patients with COPD Stratified by Disease Severity in a Commercially Insured Population. *Journal of managed care & specialty pharmacy*, *25*(2), 205–217.

8. Goyal, P., Loop, M., Chen, L., Brown, T. M., Durant, R. W., Safford, M. M., & Levitan, E. B. (2018). Causes and Temporal Patterns of 30-Day Readmission Among Older Adults Hospitalized With Heart Failure With Preserved or Reduced Ejection Fraction. *Journal of the American Heart Association*, *7*(9), e007785.

9. Angraal, S., Khera, R., Zhou, S., Wang, Y., Lin, Z., Dharmarajan, K., Desai, N. R., Bernheim, S. M., Drye, E. E., Nasir, K., Horwitz, L. I., & Krumholz, H. M. (2018). Trends in 30-Day Readmission Rates for Medicare and Non-Medicare Patients in the Era of the Affordable Care Act. *The American journal of medicine*, *131*(11), 1324–1331.e14.

10. Rhee, C., Chiotos, K., Cosgrove, S. E., Heil, E. L., Kadri, S. S., Kalil, A. C., Gilbert, D. N., Masur, H., Septimus, E. J., Sweeney, D. A., Strich, J. R., Winslow, D. L., & Klompas, M. (2021). Infectious Diseases Society of America Position Paper: Recommended Revisions to the National Severe Sepsis and Septic Shock Early Management Bundle (SEP-1) Sepsis Quality Measure. *Clinical infectious diseases : an official publication of the Infectious Diseases Society of America*, *72*(4), 541–552.

11. Kim, D. H., Lu, N., Ma, R., Kim, Y. S., Kim, R. H., Wang, S., Wu, J., Won, S. M., Tao, H., Islam, A., Yu, K. J., Kim, T. I., Chowdhury, R., Ying, M., Xu, L., Li, M., Chung, H. J., Keum, H., McCormick, M., Liu, P., … Rogers, J. A. (2011). Epidermal electronics. *Science (New York, N.Y.)*, *333*(6044), 838–843.

12. Xu, S., Jayaraman, A., & Rogers, J. A. (2019). Skin sensors are the future of health care. *Nature*, *571*(7765), 319–321.

13. Abraham, W. T., Adamson, P. B., Bourge, R. C., Aaron, M. F., Costanzo, M. R., Stevenson, L. W., Strickland, W., Neelagaru, S., Raval, N., Krueger, S., Weiner, S., Shavelle, D., Jeffries, B., Yadav, J. S., & CHAMPION Trial Study Group (2011). Wireless pulmonary artery haemodynamic monitoring in chronic heart failure: a randomised controlled trial. *Lancet (London, England)*, *377*(9766), 658–666.

14. Abraham, W. T., & Perl, L. (2017). Implantable Hemodynamic Monitoring for Heart Failure Patients. *Journal of the American College of Cardiology*, *70*(3), 389–398.

15. Abraham, W. T., Stevenson, L. W., Bourge, R. C., Lindenfeld, J. A., Bauman, J. G., Adamson, P. B., & CHAMPION Trial Study Group (2016). Sustained efficacy of pulmonary artery pressure to guide adjustment of chronic heart failure therapy: complete follow-up results from the CHAMPION randomised trial. *Lancet (London, England)*, *387*(10017), 453–461.

16. Chaudhry, S. I., Mattera, J. A., Curtis, J. P., Spertus, J. A., Herrin, J., Lin, Z., Phillips, C. O., Hodshon, B. V., Cooper, L. S., & Krumholz, H. M. (2010). Telemonitoring in patients with heart failure. *The New England journal of medicine*, *363*(24), 2301–2309.

17. Ashouri, H., Orlandic, L., & Inan, O. T. (2016). Unobtrusive Estimation of Cardiac Contractility and Stroke Volume Changes Using Ballistocardiogram Measurements on a High Bandwidth Force Plate. *Sensors (Basel, Switzerland)*, *16*(6), 787.

18. Etemadi, M., Inan, O. T., Giovangrandi, L., & Kovacs, G. T. (2011). Rapid assessment of cardiac contractility on a home bathroom scale. *IEEE transactions on information technology in biomedicine : a publication of the IEEE Engineering in Medicine and Biology Society,* 15(6), 864–869.

19. Conn, N. J., Schwarz, K. Q., & Borkholder, D. A. (2019). In-Home Cardiovascular Monitoring System for Heart Failure: Comparative Study. *JMIR mHealth and uHealth*, *7*(1), e12419.

20. Inan, O. T., Migeotte, P. F., Park, K. S., Etemadi, M., Tavakolian, K., Casanella, R., Zanetti, J., Tank, J., Funtova, I., Prisk, G. K., & Di Rienzo, M. (2015). Ballistocardiography and seismocardiography: a review of recent advances. *IEEE journal of biomedical and health informatics*, *19*(4), 1414–1427.

21. Sadek, I., Biswas, J., & Abdulrazak, B. (2019). Ballistocardiogram signal processing: a review. *Health information science and systems*, *7*(1), 10.

22. Inan, O. T., Etemadi, M., Wiard, R. M., Giovangrandi, L., & Kovacs, G. T. (2009). Robust ballistocardiogram acquisition for home monitoring. *Physiological measurement*, *30*(2), 169–185.

23. Inan, O. T., Dookun Park, Giovangrandi, L., & Kovacs, G. T. (2012). Noninvasive measurement of physiological signals on a modified home bathroom scale. *IEEE transactions on bio-medical engineering*, *59*(8), 2137–2143.

24. Aydemir, V. B., Nagesh, S., Shandhi, M., Fan, J., Klein, L., Etemadi, M., Heller, J. A., Inan, O. T., & Rehg, J. M. (2020). Classification of Decompensated Heart Failure From Clinical and Home Ballistocardiography. *IEEE transactions on bio-medical engineering*, *67*(5), 1303–1313.

25. Mack, D. C., Patrie, J. T., Suratt, P. M., Felder, R. A., & Alwan, M. A. (2009). Development and preliminary validation of heart rate and breathing rate detection using a passive, ballistocardiography-based sleep monitoring system. *IEEE transactions on information technology in biomedicine : a publication of the IEEE Engineering in Medicine and Biology Society*, *13*(1), 111–120.

26. Brüser, C., Stadlthanner, K., de Waele, S., & Leonhardt, S. (2011). Adaptive beat-to-beat heart rate estimation in ballistocardiograms. *IEEE transactions on information*

technology in biomedicine : a publication of the IEEE Engineering in Medicine and Biology Society, 15(5), 778–786.

27. Paalasmaa, J., Toivonen, H., & Partinen, M. (2015). Adaptive Heartbeat Modeling for Beat-to-Beat Heart Rate Measurement in Ballistocardiograms. *IEEE journal of biomedical and health informatics*, *19*(6), 1945–1952.

28. Helfand, M., Christensen, V., & Anderson, J. (2016). Technology Assessment: Early Sense for Monitoring Vital Signs in Hospitalized Patients. In *VA Evidence Synthesis Program Evidence Briefs*. Department of Veterans Affairs (US).

29. Bennett, M. K., Shao, M., & Gorodeski, E. Z. (2017). Home monitoring of heart failure patients at risk for hospital readmission using a novel under-the-mattress piezoelectric sensor: A preliminary single centre experience. *Journal of telemedicine and telecare*, *23*(1), 60–67.

30. Zhang, J., Goode, K. M., Cuddihy, P. E., Cleland, J. G., & TEN-HMS Investigators (2009). Predicting hospitalization due to worsening heart failure using daily weight measurement: analysis of the Trans-European Network-Home-Care Management System (TEN-HMS) study. *European journal of heart failure*, *11*(4), 420–427.

31. Tobin, M. J., Chadha, T. S., Jenouri, G., Birch, S. J., Gazeroglu, H. B., & Sackner, M. A. (1983). Breathing patterns. 2. Diseased subjects. *Chest*, *84*(3), 286–294.

32. Brinkman, J. E., Toro, F., Sharma, S (2021). In *StatPearls*. (Treasure Island (FL)).

33. Brinkman, J. E., Sharma, S (2021). In *StatPearls*. (Treasure Island (FL)).

34. Tobin, M. J., Chadha, T. S., Jenouri, G., Birch, S. J., Gazeroglu, H. B., & Sackner, M. A. (1983). Breathing patterns. 1. Normal subjects. *Chest*, *84*(2), 202–205.

35. Subbe, C. P., Kruger, M., Rutherford, P., & Gemmel, L. (2001). Validation of a modified Early Warning Score in medical admissions. *QJM : monthly journal of the Association of Physicians*, *94*(10), 521–526.

36. Raschke, R. A., Agarwal, S., Rangan, P., Heise, C. W., & Curry, S. C. (2021). Discriminant Accuracy of the SOFA Score for Determining the Probable Mortality of Patients With COVID-19 Pneumonia Requiring Mechanical Ventilation. *JAMA*, *325*(14), 1469–1470.

37. Smith, G. B., Prytherch, D. R., Meredith, P., Schmidt, P. E., & Featherstone, P. I. (2013). The ability of the National Early Warning Score (NEWS) to discriminate patients at risk

of early cardiac arrest, unanticipated intensive care unit admission, and death. *Resuscitation*, *84*(4), 465–470.

38. Prytherch, D. R., Smith, G. B., Schmidt, P. E., & Featherstone, P. I. (2010). ViEWS--Towards a national early warning score for detecting adult inpatient deterioration. *Resuscitation*, *81*(8), 932–937.

39. Seymour, C. W., Liu, V. X., Iwashyna, T. J., Brunkhorst, F. M., Rea, T. D., Scherag, A., Rubenfeld, G., Kahn, J. M., Shankar-Hari, M., Singer, M., Deutschman, C. S., Escobar, G. J., & Angus, D. C. (2016). Assessment of Clinical Criteria for Sepsis: For the Third International Consensus Definitions for Sepsis and Septic Shock (Sepsis-3). *JAMA*, *315*(8), 762–774.

40. Shankar-Hari, M., Phillips, G. S., Levy, M. L., Seymour, C. W., Liu, V. X., Deutschman, C. S., Angus, D. C., Rubenfeld, G. D., Singer, M., & Sepsis Definitions Task Force (2016). Developing a New Definition and Assessing New Clinical Criteria for Septic Shock: For the Third International Consensus Definitions for Sepsis and Septic Shock (Sepsis-3). *JAMA*, *315*(8), 775–787.

41. STARR, I., HORWITZ, O., MAYOCK, R. L., & KRUMBHAAR, E. B. (1950). Standardization of the ballistocardiogram by simulation of the heart's function at necropsy; with a clinical method for the estimation of cardiac strength and normal standards for it. *Circulation*, *1*(5), 1073–1096.

42. Zhang GQ, Cui L, Mueller R, Tao S, Kim M, Rueschman M, Mariani S, Mobley D, Redline S. The National Sleep Research Resource: towards a sleep data commons. J Am Med Inform Assoc. 2018 Oct 1;25(10):1351-1358. doi: 10.1093/jamia/ocy064. PMID: 29860441; PMCID: PMC6188513.

43. Redline S, Sotres-Alvarez D, Loredo J, Hall M, Patel SR, Ramos A, Shah N, Ries A, Arens R, Barnhart J, Youngblood M, Zee P, Daviglus ML. Sleep-disordered breathing in Hispanic/Latino individuals of diverse backgrounds. The Hispanic Community Health Study/Study of Latinos. Am J Respir Crit Care Med. 2014 Feb 1;189(3):335-44. doi: 10.1164/rccm.201309-1735OC. PMID: 24392863; PMCID: PMC3977733.

44. Blackwell T, Yaffe K, Ancoli-Israel S, Redline S, Ensrud KE, Stefanick ML, Laffan A, Stone KL; Osteoporotic Fractures in Men Study Group. Associations between sleep architecture and sleep-disordered breathing and cognition in older community-dwelling men: the Osteoporotic Fractures in Men Sleep Study. J Am Geriatr Soc. 2011 Dec; 59(12):2217-25. doi: 10.1111/j.1532-5415.2011.03731.x. Epub 2011 Nov 7. PMID: 22188071; PMCID: PMC3245643.

45. Chen X, Wang R, Zee P, Lutsey PL, Javaheri S, Alcántara C, Jackson CL, Williams MA, Redline S. Racial/Ethnic Differences in Sleep Disturbances: The Multi-Ethnic Study of Atherosclerosis (MESA). Sleep. 2015 Jun 1;38(6):877-88. doi: 10.5665/sleep.4732. PMID: 25409106; PMCID: PMC4434554.

46. Quan SF, Howard BV, Iber C, Kiley JP, Nieto FJ, O'Connor GT, Rapoport DM, Redline S, Robbins J, Samet JM, Wahl PW. The Sleep Heart Health Study: design, rationale, and methods. Sleep. 1997 Dec;20(12):1077-85. PMID: 9493915.

47. Young T, Palta M, Dempsey J, Peppard PE, Nieto FJ, Hla KM. Burden of sleep apnea: rationale, design, and major findings of the Wisconsin Sleep Cohort study. WMJ. 2009 Aug;108(5):246-9. PMID: 19743755; PMCID: PMC2858234.

48. Berwick, D. M., Nolan, T. W., & Whittington, J. (2008). The triple aim: care, health, and cost. *Health affairs (Project Hope)*, *27*(3), 759–769.

49. Ferrer, R., Martin-Loeches, I., Phillips, G., Osborn, T. M., Townsend, S., Dellinger, R. P., Artigas, A., Schorr, C., & Levy, M. M. (2014). Empiric antibiotic treatment reduces mortality in severe sepsis and septic shock from the first hour: results from a guideline-based performance improvement program. *Critical care medicine*, *42*(8), 1749–1755.

50. Rhodes, A., Evans, L. E., Alhazzani, W., Levy, M. M., Antonelli, M., Ferrer, R., Kumar, A., Sevransky, J. E., Sprung, C. L., Nunnally, M. E., Rochwerg, B., Rubenfeld, G. D., Angus, D. C., Annane, D., Beale, R. J., Bellinghan, G. J., Bernard, G. R., Chiche, J. D., Coopersmith, C., De Backer, D. P., … Dellinger, R. P. (2017). Surviving Sepsis Campaign: International Guidelines for Management of Sepsis and Septic Shock: 2016. *Intensive care medicine*, *43*(3), 304–377.

51. Dempster, A. P., Laird, N. M., & Rubin, D. B. (1977) Maximum likelihood from incomplete data via the EM algorithm. *J. R. Stat. Soc Ser. B Methodological,* 39, 1–38

52. Durbin, J. & Koopman, S. J. Time Series Analysis by State Space Methods (2001). Oxford Univ. Press